solvents for LC-MS were purchased from Sigma-Aldrich Japan. All of the other chemicals were of reagent or HPLC grade and were used without further purification.

**Plant Material** The dried gardenia fruits, defined as the fruits of *Gardenia jasminoides*, were purchased from Uchida Wakanyaku Co., Ltd., Japan, in July 2004. The crude drug name was Gardeniae Fructus (Serial No.: VMAMQ), and the voucher specimen (GJ 72004) was deposited at Division of Food Additives in National Institute of Health Sciences.

**Extraction and Isolation** Gardenia yellow was extracted by stirring dried gardenia fruits (1 kg) with 50% aqueous ethanol at ambient temperature in the dark for 2 h. The part of extracted gardenia yellow (2.25 g) was subsequently fractionated on a Diaion HP-20 column (40 mm i.d.×250 mm) by successive elution with 0—100% MeOH. The 60—70% methanol eluate was then concentrated *in vacuo* and the residue was loaded into a preparative LC-MS system.[6] The conditions were as follows: column, Waters XTerra® Prep MS $C_{18}$ (5 $\mu$m, 19 mm i.d.×100 mm); mobile phase, $H_2O$ : MeOH = 58 : 42; flow rate, 10 ml/min; make-up liquid, MeOH 1.0 ml/min; injection volume, 200 $\mu$l; and detection and collection trigger, ESI (pos.) *m/z* 999.5. The electrospray source ran at a 3.0 kV capillary voltage, with 120 and 350 °C source and desolvation temperatures, respectively, and with 350 and 60 l/h desolvation and cone gases, respectively. The cone voltage was 50 V. Full-scan acquisition between *m/z* 100 and 2000 was performed at a scan speed of 0.3 s/scan, with a 0.1-s inter-scan delay. The solvent delivered to the electrospray interface was split in a 1 : 4 ratio, delivering around 200 $\mu$l/min to the interface. The peaks of crocin (**1**) (retention time ($t_R$) 15.3 min) and neocrocin A (**2**) ($t_R$ 19.0 min) were each fractionated and concentrated *in vacuo* at <40 °C. The overall procedure was repeated approximately 25 times to afford 220 mg of crocin (**1**) and 18 mg of neocrocin A (**2**).

**Crocin (1)**[2] Red amorphous powder. IR (KBr) $\nu_{max}$ cm$^{-1}$: 1069, 1227, 1271, 1577, 1699, 2920, 3398. UV/Vis (MeOH) $\lambda_{max}$ (log $\varepsilon$): 433 (4.49), 458 (4.46), 259 (3.65). HR-ESI-MS *m/z*: 999.3674 $[M+Na]^+$ (Calcd for $C_{44}H_{64}O_{24}Na$: 999.3685). $^1$H (800 MHz)- and $^{13}$C (200 MHz)-NMR spectral data: see Table 1.

**Neocrocin A (2)** Red amorphous powder. IR (KBr) $\nu_{max}$ cm$^{-1}$: 1023, 1227, 1270, 1578, 1702, 2918, 3375. UV/Vis (MeOH) $\lambda_{max}$ (log $\varepsilon$): 432 (4.73), 457 (4.69), 258 (3.97). HR-ESI-MS *m/z* 999.3707 $[M+Na]^+$ (Calcd for $C_{44}H_{64}O_{24}Na$, 999.3685). $^1$H (800 MHz)- and $^{13}$C (200 MHz)-NMR spectral data: see Table 1.

**Crocetin Dimethyl Ester (3)** Methanolysis of **2** (10 mg) with 5% HCl methanol at room temperature for 50 h resulted in red amorphous powder (**3**, 3 mg) after purification by Silica gel column chromatography (EtOAc : hexane = 2 : 3). ESI-MS *m/z*: 327 $[M-H]^-$. $^1$H-NMR ($CDCl_3$, 500 MHz) $\delta$: 1.98 (6H, s, H-20, 20′), 1.99 (6H, s, H-19, 19′), 3.75 (6H, s, MeO×2), 6.35 (2H, br d, $J$=10.0 Hz, H-14, 14′), 6.53 (2H, dd, $J$=11.0, 15.0 Hz, H-11, 11′), 6.60 (2H, d, $J$=15.0 Hz, H-12, 12′), 6.70 (2H, dd, $J$=3.0, 8.0 Hz, H-15, 15′), 7.28 (2H, dd, $J$=1.4, 11.0 Hz, H-10, 10′); $^{13}$C-NMR ($CDCl_3$, 125 MHz) $\delta$: 12.87 (C-20, 20′), 12.99 (C-19, 19′), 51.92 (MeO×2), 123.88 (C-11, 11′), 126.48 (C-9, 9′), 131.40 (C-15, 15′), 135.43 (C-14, 14′), 136.79 (C-13, 13′), 138.97 (C-10, 10′), 143.84 (C-12, 12′), 169.02 (C-8, 8′).

**Peracetylated Crocin (1a) and Neocrocine A (2a)** Peracetylation of gardenia yellow (1.0 g) was carried out with $Ac_2O$/pyridine (cat. DMAP), affording peracetylated crocin (**1a**, 1.5 g) ($t_R$ 26.0 min) and the a isomer of neocrocin A (**2a**, 7.4 mg) ($t_R$ 27.9 min) using preparative LC/MS[6] under the following conditions: column, YMC J'sphere ODS-L80 (5 $\mu$m, 20 mm i.d.×250 mm); mobile phase, $H_2O$ : MeCN = 42 : 58; flow rate, 10 ml/min; make-up liquid, MeOH 1.0 ml/min; injection volume, 200 $\mu$l; detection and collection trigger, ESI (positive mode), *m/z* 1587.5. The overall procedure was repeated approximately 30 times. The $\beta$ isomer of peracetylated **2** could not be isolated because of overlapping with the peak of **1a**.

**1a** red amorphous powder. IR (KBr) $\nu_{max}$ cm$^{-1}$: 1063, 1222, 1371, 1615, 1751, 2944. UV/Vis (MeOH) $\lambda_{max}$ (log $\varepsilon$): 436 (4.95), 462 (4.92), 260 (4.05). HR-ESI-MS *m/z*: 1587.5156 $[M+Na]^+$ (Calcd for $C_{72}H_{92}O_{38}Na$: 1587.5164). **2a** (an $\alpha$ isomer): red amorphous powder. IR (KBr) $\nu_{max}$ cm$^{-1}$: 1038, 1223, 1375, 1637, 1752, 2945. UV/Vis (MeOH) $\lambda_{max}$ (log $\varepsilon$): 438 (4.81), 460 (4.77), 260 (4.05). HR-ESI-MS *m/z* 1587.5192 $[M+Na]^+$ (Calcd for $C_{72}H_{92}O_{38}Na$: 1587.5164); $^1$H (800 MHz)- and $^{13}$C (200 MHz)-NMR spectral data of **1a** and **2a**: see Table 2.

## References and Notes


1) Present address: *School of Food and Nutritional Sciences, University of Shizuoka; 52–1 Yada, Suruga, Shizuoka 422–8526, Japan.*
2) Calsteren M. V., Bissonnette M. C., Cormier F., Dufresne C., Ichi T., LeBlanc J. C. Y., Perreault D., Roewer I., *J. Agric. Food Chem.*, **45**, 1055—1061 (1997).
3) Carmona M., Zalacain A., Sánchez A. M., Novella J. L., Alonso G. L., *J. Agric. Food Chem.*, **54**, 973—979 (2006).
4) Ichi T., Higashimura Y., Katayama T., Koda T., Shimizu T., Tada M. J., *Jpn. Soc. Food Sci. Technol.*, **42**, 776—783 (1995).
5) Pfister S., Meyer P., Steck A., Pfander H., *J. Agric. Food Chem.*, **44**, 2612—2615 (1996).
6) Sato K., Sugimoto N., Ohta M., Yamazaki T., Maitani T., Tanamoto K., *Food Add. Contam.*, **20**, 1015—1022 (2003).
7) Kawahara N., Tamura T., Inoue M., Hosoe T., Kawai K., Sekita S., Satake M., Goda Y., *Phytochemistry*, **65**, 2577—2581 (2004).

SHORT COMMUNICATION

# Effects of possible endocrine disruptors on MyD88-independent TLR4 signaling

Takahiro Ohnishi, Tomohisa Yoshida, Arisa Igarashi, Masashi Muroi & Ken-ichi Tanamoto

Division of Microbiology, National Institute of Health Sciences, Setagaya, Tokyo, Japan

**Correspondence:** Ken-ichi Tanamoto, Division of Microbiology, National Institute of Health Sciences, 1-18-1 Kamiyoga, Setagaya, Tokyo 158-8501, Japan. Tel.: +81 3 3700 1141, ext. 321; fax: +81 3 3700 9484; e-mail: tanamoto@nihs.go.jp

Received 3 July 2007; revised 13 September 2007; accepted 8 October 2007.
First published online 20 December 2007.

DOI:10.1111/j.1574-695X.2007.00355.x

Editor: Patrick Brennan

**Keywords**
endocrine disruptors; IFN-β; lipopolysaccharide; bacterial lipoprotein; macrophage.

## Abstract

Endocrine disrupting chemicals (EDCs) may potentially worsen infectious diseases because EDCs disturb human immune function by interfering with endocrine balance. To evaluate the influence of EDCs on the innate immune function of macrophages, we investigated the effects of 37 possible EDCs on lipopolysaccharide-induced activation of the IFN-β promoter. Alachlor, atrazine, benomyl, bisphenol A, carbaryl, diethyl phthalate, dipropyl phthalate, kelthane, kepone, malathion, methoxychlor, octachlorostyrene, pentachlorophenol, nonyl phenol, *p*-octylphenol, simazine and ziram all inhibited the activation. Kepone and ziram showed strong inhibitory effects. Aldicarb, amitrole, benzophenone, butyl benzyl phthalate, 2,4-dichlorophenoxy acetic acid, dibutyl phthalate, 2,4-dichlorophenol, dicyclohexyl phthalate, diethylhexyl adipate, diethylhexyl phthalate, dihexyl phthalate, di-*n*-pentyl phthalate, methomyl, metribuzin, nitrofen, 4-nitrotoluene, permethrin, trifluralin, 2,4,5-trichlorophenoxyacetic acid and vinclozolin had no significant effects at 100 μM. These results indicate that some agrochemicals and resin-related chemicals may potentially inhibit macrophage function, which suggests that endocrine disruptors may influence the development of infectious diseases.

Endocrine disrupting chemicals (EDCs) are exogenous substances that mimic, antagonize, impair, enhance or inhibit the actions of endogenous hormones and in turn cause abnormalities of growth, reproduction, development, behavior and immune function, or cause malignant tumors (Safe *et al.*, 1998; Schrenk, 1998; Eskenazi *et al.*, 2000). EDCs exert their activity at multiple sites by multiple mechanisms. Receptor-mediated mechanisms have been well studied, but other mechanisms including effects on hormone synthesis, transport and metabolism are also involved (Masuyama *et al.*, 2000; Inoshita *et al.*, 2003). However, the secondary effects of EDCs, such as the influence on infectious diseases, are not well known. Infectious diseases are caused by microbial invasion. The human body is equipped with a complicated immune system to cope with microbial invasion. Disorder of this well-organized immune system may lead to the development of serious infectious diseases; therefore, it is possible that EDCs may worsen the effects of infectious diseases because any disorder of the endocrine system seriously disturbs immune function. Macrophages are recognized as an important component of the host immune system, and are activated by microbial components, especially by lipopolysaccharide (Fujihara *et al.*, 2003). Previously, we investigated the effects of various possible EDCs on macrophage activation and found that some EDCs strongly inhibit lipopolysaccharide-induced TNF-α and nitric oxide production by macrophages (Hong *et al.*, 2004). Since the activation of the transcription factor nuclear factor (NF)-κB is essential for tumour necrosis factor α (TNF-α) and nitric oxide production, we further investigated the effects of these possible EDCs on bacterial component-induced activation of NF-κB and found that reduced NF-κB activity is partly involved in the inhibition of TNF-α and nitric oxide production (Igarashi *et al.*, 2006). It is well known that lipopolysaccharide activates both MyD88-dependent and MyD88-independent pathways, and both signaling pathways are involved in lipopolysaccharide-induced production of TNF-α and nitric oxide (Akira & Takeda, 2004). The activation of both pathways leads to the activation of NF-κB, while the activation of the IFN-β promoter is induced only by the MyD88-independent pathway. Thus, to assess the influence of EDCs on the lipopolysaccharide-mediated MyD88-independent pathway, in the present study we have investigated the effects of possible

EDCs on lipopolysaccharide-induced activation of the IFN-β promoter. The chemicals were selected from the SPEED'98 list (http://www.env.go.jp/en/chemi/ed.html; SPEED'98 has been revised and 'Perspectives on Endocrine Disrupting Effects of Substances – ExTEND 2005' has been issued during the preparation of this manuscript) issued by the Ministry of the Environment of Japan depending on their availability and water solubility. Chemicals showing higher cellular toxicity were excluded. We selected 37 chemicals (described as EDCs in this study) that are suspected of having endocrine-disrupting effects from among agrochemicals and resin-related chemicals, and their abbreviations are shown in Table 1. We used the mouse macrophage cell line RAW 264, stably carrying an IFN-β-dependent luciferase reporter gene, to systematically compare the effect of each chemical on lipopolysaccharide-induced activation of the MyD88-independent pathway. Cells were incubated with 100 μM of each chemical followed by lipopolysaccharide, and then the reporter activity was measured. The reporter activity was normalized to the protein concentration for the compensation of difference in cell numbers and viabilities between wells. Table 1 summarizes the results. Seventeen chemicals: ACL, ATZ, BML, BPA, NAC, DEP, DPrP, KLT, KPN, MAT, DMDT, OCS, PCP, NNP, OTP, CAT and ZRM, inhibited lipopolysaccharide-induced activation of the IFN-β promoter. A strong inhibitory effect was observed with KPN and ZRM. No significant enhancement of lipopolysaccharide-induced activation of the IFN-β promoter was observed with any of the chemicals. We next examined the concentration dependency of the 16 chemicals that affected lipopolysaccharide-induced activation of IFN-β (Fig. 1). The effects of CAT could not be evaluated because of its poor solubility. Although the effects of OCS, DEP and DprP were weak even at 200 μM, all of the EDCs tested inhibited the activation in a concentration-dependent manner.

In the present study, we examined the effects of 37 chemicals suspected of having endocrine-disrupting properties on lipopolysaccharide-induced activation of the IFN-β promoter, to evaluate the effect of EDCs on macrophage activation. We found that 17 of the chemicals inhibited IFN-β promoter activation (Table 1). No chemicals by themselves induced IFN-β promoter activation nor enhanced lipopolysaccharide-induced activation. In this study, the chemicals we examined are classified as agrochemicals and resin-related chemicals. We found that stronger inhibitory activity was observed with agrochemicals. Most of the chemicals showed their effects at a concentration range of 50–200 μM, which may be higher than the levels that typically occur in the environment. In the natural environment, humans are exposed to multiple chemicals chronically, and the bioaccumulation and synergistic effects of these chemicals are not well understood; therefore, it may be possible that chronic exposure to even low levels of these chemicals could have some impact on human health.

**Table 1.** Effects of possible EDCs on lipopolysaccharide-induced activation of IFN-β promoter

| Chemicals | Abbreviation | Class | % Response |
|---|---|---|---|
| Alachlor | ACL | a | 43.5 ± 3.91** |
| Aldicarb | ACB | a | 104.9 ± 2.38 |
| Amitrole | ATA | a | 92.3 ± 6.20 |
| Atrazine | ATZ | a | 49.3 ± 5.93* |
| Benomyl | BML | a | 34.7 ± 6.31 |
| Benzophenone | BZP | r | 84.1 ± 7.31 |
| Butyl benzyl phthalate | BBP | r | 104.8 ± 10.64 |
| Bisphenol A | BPA | r | 59.2 ± 5.57* |
| Carbaryl | NAC | a | 78.0 ± 6.99* |
| 2,4-Dichlorophenoxy acetic acid | 2,4-D | a | 109.8 ± 15.90 |
| Dibutyl phthalate | DBP | r | 99.7 ± 5.23 |
| 2,4-Dichlorophenol | DCP | r | 74.4 ± 6.34 |
| Dicyclohexyl phthalate | DCHP | r | 98.3 ± 18.46 |
| Diethylhexyl adipate | DOA | r | 80.5 ± 4.69 |
| Diethylhexyl phthalate | DOP | r | 82.5 ± 4.70 |
| Diethyl phthalate | DEP | r | 62.9 ± 7.04* |
| Dihexyl phthalate | DHP | r | 81.0 ± 4.15 |
| Di-*n*-pentyl phthalate | DPP | r | 82.2 ± 9.60 |
| Dipropyl phthalate | DPrP | r | 72.4 ± 1.86** |
| Kelthane | KLT | a | 30.7 ± 6.24** |
| Kepone | KPN | a | 5.2 ± 0.54** |
| Malathion | MAT | a | 73.6 ± 4.45* |
| Methomyl | MTM | a | 96.1 ± 7.96 |
| Methoxychlor | DMDT | a | 81.5 ± 2.08* |
| Metribuzin | MTB | a | 86.3 ± 5.23 |
| Nitrofen | NIP | r | 104.0 ± 6.16 |
| 4-Nitrotoluene | NTT | r | 111.7 ± 4.90 |
| Octachlorostyrene | OCS | r | 77.2 ± 1.59** |
| Pentachlorophenol | PCP | a | 61.4 ± 4.80** |
| Nonyl phenol | NNP | r | 52.8 ± 2.61** |
| *p*-Octylphenol | OTP | r | 56.4 ± 1.08** |
| Permethrin | PMT | a | 100.1 ± 7.86 |
| Simazine | CAT | a | 72.9 ± 1.40** |
| Trifluralin | TFR | a | 87.2 ± 5.22 |
| 2,4,5-Trichlorophenoxyacetic acid | 2,4,5-T | a | 94.6 ± 5.13 |
| Vinclozolin | VCZ | a | 87.4 ± 5.64 |
| Ziram | ZRM | a | 0.2 ± 0.09** |

Values are expressed as percent (mean ± SEM) of respective control where no EDC treatment was performed. Data are from at least three independent experiments. All chemicals were used at 100 mM.

*$P < 0.05$.

**$P < 0.01$, compared with the respective control by paired Student's *t*-test.

a, Agrochemicals; r, resin-related chemicals.

We previously reported (Hong *et al.*, 2004; Igarashi *et al.*, 2006) that ACL, NAC, CAT, NNP and OTP, which inhibited either lipopolysaccharide-induced TNF-α or nitric oxide production by macrophages, also inhibited lipopolysaccharide-induced NF-κB activation. In the present study, we found that these chemicals also inhibit lipopolysaccharide-

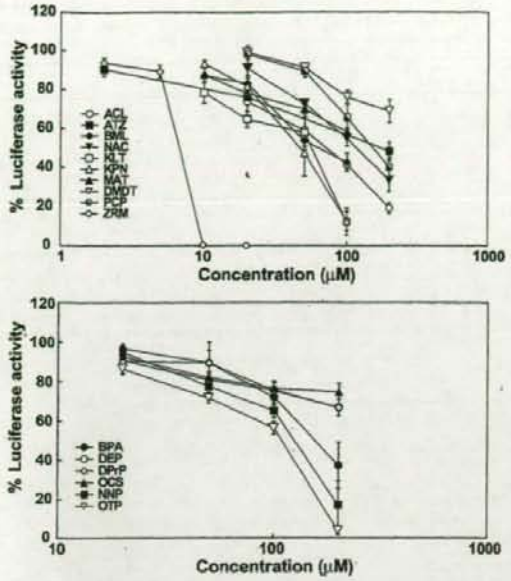


**Fig. 1.** Concentration-dependent effects of possible EDCs on lipopolysaccharide-induced activation of the IFN-β promoter. RAW 264 cells stably carrying an IFN-β-dependent luciferase reporter gene were stimulated with 10 ng mL$^{-1}$ of lipopolysaccharide for 6 h with or without the indicated concentrations of EDCs, and luciferase activity was then measured. Values are means ± SEM from at least three independent experiments. The reporter activity in response to lipopolysaccharide alone is expressed as 100%.

induced IFN-β promoter activity. Since both MyD88-dependent and MyD88-independent pathways are essential for the production of TNF-α and nitric oxide, the inhibition of both NF-κB and IFN-β promoter activity by these chemicals may be involved in the inhibitory effects on TNF-α and nitric oxide production. Most, but not all, of the chemicals that inhibited lipopolysaccharide-induced IFN-β promoter activity also possessed inhibitory activity on lipopolysaccharide-induced NF-κB activation (Igarashi *et al.*, 2006). ACL and NAC, even at 370 and 500 μM, respectively, did not significantly affect SV40 promoter-based reporter activity (data not shown), indicating that the effect of these chemicals on IFN-β promoter and NF-κB activity was not nonspecific. Although the mechanism by which these chemicals inhibit both activities is unknown, activation of NF-κB and stimulation of MyD88-independent signaling are essential to the innate immune function. It is, therefore, of concern that these chemicals may have the potential to exacerbate infectious diseases.

## Acknowledgement

This work was supported in part by a grant from the Ministry of the Environment, Japan.

## References

Akira S & Takeda K (2004) Toll-like receptor signalling. *Nat Rev Immunol* **4**: 499–511.

Eskenazi B, Mocarelli P, Warner M, Samuels S, Vercellini P, Olive D, Needham L, Patterson D & Brambilla P (2000) Seveso Women's Health Study: a study of the effects of 2,3,7,8-tetrachlorodibenzo-*p*-dioxin on reproductive health. *Chemosphere* **40**: 1247–1253.

Fujihara M, Muroi M, Tanamoto K, Suzuki T, Azuma H & Ikeda H (2003) Molecular mechanisms of macrophage activation and deactivation by lipopolysaccharide: roles of the receptor complex. *Pharmacol Ther* **100**: 171–194.

Hong CC, Shimomura-Shimizu M, Muroi M & Tanamoto K (2004) Effect of endocrine disrupting chemicals on lipopolysaccharide-induced tumor necrosis factor-alpha and nitric oxide production by mouse macrophages. *Biol Pharm Bull* **27**: 1136–1139.

Igarashi A, Ohtsu S, Muroi M & Tanamoto K (2006) Effects of possible endocrine disrupting chemicals on bacterial component-induced activation of NF-kappaB. *Biol Pharm Bull* **29**: 2120–2122.

Inoshita H, Masuyama H & Hiramatsu Y (2003) The different effects of endocrine-disrupting chemicals on estrogen receptor-mediated transcription through interaction with coactivator TRAP220 in uterine tissue. *J Mol Endocrinol* **31**: 551–561.

Masuyama H, Hiramatsu Y, Kunitomi M, Kudo T & MacDonald PN (2000) Endocrine disrupting chemicals, phthalic acid and nonylphenol, activate Pregnane X receptor-mediated transcription. *Mol Endocrinol* **14**: 421–428.

Safe S, Wang F, Porter W, Duan R & McDougal A (1998) Ah receptor agonists as endocrine disruptors: antiestrogenic activity and mechanisms. *Toxicol Lett* **102–103**: 343–347.

Schrenk D (1998) Impact of dioxin-type induction of drug-metabolizing enzymes on the metabolism of endo- and xenobiotics. *Biochem Pharmacol* **55**: 1155–1162.

Uncorrected Version. Published on December 10, 2007 as DOI:10.1189/jlb.0907629

# TRAF6 distinctively mediates MyD88- and IRAK-1-induced activation of NF-κB

Masashi Muroi and Ken-ichi Tanamoto[1]

*Division of Microbiology, National Institute of Health Sciences, Tokyo, Japan*

**Abstract: MyD88 and IL-1R-associated kinase 1 (IRAK-1) play crucial roles as adaptor molecules in signal transduction of the TLR/IL-1R superfamily, and it is known that expression of these proteins leads to the activation of NF-κB in a TNFR-associated factor 6 (TRAF6)-dependent manner. We found in this study, however, that a dominant-negative mutant of TRAF6, lacking the N-terminal RING and zinc-finger domain, did not inhibit IRAK-1-induced activation of NF-κB in human embryo kidney 293 cells, although the TRAF6 mutant strongly suppressed the MyD88-induced activation. The dominant-negative mutant of TRAF6 did not affect the IRAK-1-induced activation, regardless of the expression level of IRAK-1. In contrast, small interfering RNA silencing of TRAF6 expression inhibited MyD88-induced and IRAK-1-induced activation, and supplementation with the TRAF6 dominant-negative mutant did not restore the IRAK-1-induced activation. Expression of IRAK-1, but not MyD88, induced the oligomerization of TRAF6, and IRAK-1 and the TRAF6 dominant-negative mutant were associated with TRAF6. These results indicate that TRAF6 is involved but with different mechanisms in MyD88-induced and IRAK-induced activation of NF-κB and suggest that TRAF6 uses a distinctive mechanism to activate NF-κB depending on signals. *J. Leukoc. Biol.* 83: 000–000; 2008.**

***Key Words:*** *Toll-like receptor · IL-1 receptor · lipopolysaccharide*

## INTRODUCTION

TLR/IL-1R family members share common intracellular signaling proteins including MyD88, the IL-1R-associated kinase (IRAK) family, and TNFR-associated factor 6 (TRAF6) [1, 2]. Ligand binding triggers the recruitment of MyD88 to the Toll/IL-1R (TIR) domain of TLR/IL-1R via a homophilic TIR–TIR interaction, which in turn, recruits IRAK-4 and IRAK-1 into the receptor complex. IRAK-4 does not bind IRAK-1 directly but is recruited into the complex through binding with MyD88. This allows IRAK-1 and IRAK-4 to come in close proximity, which induces IRAK-4 to phosphorylate IRAK-1 [3], probably triggering autophosphorylation of IRAK-1. Autophosphorylated IRAK-1 interacts with TRAF6 [4], leading to the activation of NF-κB [1].

MyD88 is known as a universal adaptor molecule that interacts with IL-1R and most of TLRs. MyD88 consists of an N-terminal death domain separated by a short internal linker from a C-terminal TIR domain, which is necessary for the interaction with the TIR domain of TLR/IL-1R. The death domain and the internal linker domain have been implicated in the interaction with IRAK-1 and IRAK-4, respectively [5]. IRAK-1 consists of an N-terminal death domain, which is involved in the binding of MyD88 [6], and a central serine/threonine kinase domain. The C-terminal region of IRAK-1 contains three potential TRAF6-binding sites, and mutation of the amino acids ($Glu^{544}$, $Glu^{587}$, $Glu^{706}$) in these sites to alanine greatly reduces activation of NF-κB [7]. The death domain and the internal domain between the death domain and the kinase domain of IRAK-1 are also involved in binding TRAF6. The N-terminal region (death domain and internal domain) and the first half of the C-terminal region are sufficient for IL-1-induced activation of NF-κB [8].

It is known that all of MyD88, IRAK-1, and TRAF6 are involved in TLR/IL-R signaling to activate NF-κB. However, it is still enigmatic how these molecules lead to the activation of NF-κB [9]. Polyubiquitination of TRAF6 is reportedly important for TLR/IL-1R signaling [10]. TRAF6 itself functions, in conjunction with the ubiquitin-conjugating enzyme complex Ubc13-Uev1A, as a ubiquitin ligase that catalyzes the formation of unique $Lys^{63}$-linked polyubiquitin chains [11, 12]. TRAF6 catalyzes $Lys^{63}$-linked polyubiquitination on TRAF6 itself, and the polyubiquitinated TRAF6 activates NF-κB signaling proteins by a proteasome-independent mechanism [11, 12]. On the other hand, it has also been reported that oligomerization of TRAF6 induces activation of NF-κB [12, 13]. However, the relationship between the polyubiquitination and the oligomerization is unknown, and the role of MyD88 and IRAK-1 in these events is still ambiguous. We report here for the first time in our knowledge that TRAF6 distinctively mediates MyD88-induced and IRAK-1-induced activation of NF-κB and that only IRAK-1 leads to oligomerization of TRAF6.

[1] Correspondence: Division of Microbiology, National Institute of Health Sciences, 1-18-1 Kamiyoga, Setagaya, Tokyo 158-8501, Japan. E-mail: tanamoto@nihs.go.jp

Received September 13, 2007; revised November 9, 2007; accepted November 12, 2007.

doi: 10.1189/jlb.0907629

## MATERIALS AND METHODS

### Cell culture and reagents

The human embryo kidney (HEK)293 cell line (obtained from the Human Science Research Resources Bank, Tokyo, Japan) was grown in DMEM (Invitrogen, Carlsbad, CA, USA), supplemented with 10% (v/v) heat-inactivated FCS (Invitrogen), penicillin (100 U/ml), and streptomycin (100 μg/ml). *Escherichi coli* O111:B4 LPS was obtained from Sigma-Aldrich (St. Louis, MO, USA) and was repurified according to the method described by Hirschfeld et al. [14]. A stable cell population expressing FLAG-tagged TRAF6 and equine infectious anaemia virus (EIAV)-tagged TRAF6 was established as follows. After linearizing with *Bgl*II, expression plasmids encoding FLAG-tagged TRAF6 and EIAV-tagged TRAF6 were transfected into HEK293 cells by the calcium phosphate precipitation method. Transfected cells were selected for G418 resistance at a concentration of 1 mg/ml. An antiserum against the EIAV-tag epitope (amino acid sequence: ADRRIPGTAEE) was a kind gift from Dr. Nancy Rice (National Cancer Institute-Frederick Cancer Research and Development Center, Frederick, MD, USA). Antibodies against TRAF6 (H-274, Santa Cruz Biotechnology, Santa Cruz, CA, USA) and FLAG-epitope (M2, Sigma-Aldrich) were used. Anti-FLAG M2 affinity gel was from Sigma-Aldrich. A TRAF6 small interfering (si)RNA oligo (CCACGAAGAGAUAAUGGAUdTdT) [15] was synthesized by Qiagen (Valencia, CA, USA).

### Plasmids

The coding regions of human MyD88 and IκB kinase β (IKKβ) were amplified by RT-PCR from total RNA prepared from human spleen (OriGene Technologies, Rockville, MD, USA) and THP-1 cells, respectively. The coding region of human TRAF6 was amplified from a human spleen cDNA library (Clontech, Palo Alto, CA, USA). A plasmid containing human IRAK-1 cDNA was obtained from the Mammalian Gene Collection. Deletions found in the IRAK-1 plasmid were corrected by PCR-mediated mutagenesis. The coding regions of all of these constructs were subcloned into mammalian expression vectors containing the N-terminal EIAV-tag and FLAG-tag epitope sequences. NF-κB-dependent luciferase reporter plasmid endothelial leukocyte adhesion molecule ligand (pELAM-L) was described previously [16]. All mutant plasmids were created by PCR-mediated mutagenesis, and mutations were confirmed by DNA sequencing.

### NF-κB reporter assay, RNA interference, immunoprecipitation, and immunoblotting

The NF-κB-dependent luciferase reporter assay was performed as described elsewhere [17]. Briefly, HEK293 cells ($2–5\times10^5$ cells) were plated in six-well plates and transfected the following day by the calcium phosphate precipitation method with the indicated plasmids: 0.2 μg pELAM-L and 5 ng phRL-TK (Promega, Madison, WI, USA), for normalization. At 24–32 h after transfection, cellular extracts were prepared by adding a lysis buffer [10 mM HEPES-KOH, pH 7.9, 10 mM KCl, 5 mM EDTA, 40 mM β-glycerophosphate, 0.5% Nonidet P-40 (NP-40), 30 mM NaF, 1 mM $Na_3VO_4$, 100 nM okadaic acid] containing a protease inhibitor cocktail (Roche Diagnostics, Mannheim, Germany). Reporter gene activity was measured with a portion of the cellular extract, according to the manufacturer's (Promega) instruction. To another portion of the cellular extract, anti-FLAG M2-agarose (Sigma-Aldrich) was added, and the mixture was incubated at 4°C for 1 h. The agarose was washed three times with PBS containing 0.5% NP-40, and bound proteins were subsequently eluted from the agarose by incubating with 0.1% SDS. The resulting supernatant was subjected to SDS-PAGE. Proteins were transferred to a polyvinylidene difluoride membrane (Immobilon-P, Millipore, Bedford, MA, USA) and subjected to immunoblotting with the indicated antibodies. The signals were visualized by using an enhanced chemiluminescence system (GE Healthcare Bio-sciences, Piscataway, NJ, USA). For RNA interference, HEK293 cells ($1–3\times10^5$ cells) were plated in six-well plates and transfected the following day by the calcium phosphate precipitation method with the indicated amounts of a siRNA oligo. On the following day after the first transfection, reporter plasmids indicated expression plasmids, and the siRNA oligo were transfected further as described above. The transfected amount of siRNA oligo was normalized by supplementing an unrelated oligo. At 24–32 h after the second transfection, cellular extracts were prepared, and reporter activities were determined as above.

## RESULTS

### A dominant-negative mutant of TRAF6 inhibits MyD88-induced but not IRAK-1-induced activation of NF-κB

To explore the involvement of TRAF6 in MyD88- and IRAK-1-induced activation of NF-κB, we examined the effects of a dominant-negative mutant of TRAF6. It is well known that the deletion of the N-terminal RING and zinc-finger domain (aa 1–288) of TRAF6 abolishes the ability of TRAF6 to mediate IL-1- and LPS-induced activation of NF-κB [18] and that the N-terminal deletion mutant acts as a dominant-negative mutant [4]. Thus, this N-terminal deletion mutant of TRAF6 was expressed with MyD88 or IRAK-1 and measured NF-κB-dependent reporter activity in HEK293 cells (**Fig. 1**). As expected, the expression of MyD88 activated NF-κB, and the coexpression of the TRAF6 deletion mutant inhibited this activation in a dose-dependent manner. However, IRAK-1-induced activation of NF-κB was surprisingly unaffected by coexpression of the deletion mutant. On the other hand, MyD88- and IRAK-1-induced activation of NF-κB were inhibited by a kinase-dead mutant (K44A) of IKKβ, indicating that the activation induced by MyD88 and IRAK-1 is IKK-dependent. The expression levels of MyD88 and IRAK-1 were not affected by coexpression of the TRAF6 deletion mutant (Fig. 1, lower panels).

To confirm the inability of the TRAF6 deletion mutant to inhibit IRAK-1-induced activation of NF-κB, the effect of the deletion mutant was examined further by changing the expression levels of MyD88 and IRAK-1 (**Fig. 2**). The TRAF6 deletion mutant inhibited MyD88-induced activation of NF-κB (Fig. 2A, right), irrespective of the MyD88 expression level (Fig. 2B); however, IRAK-1-induced activation was not af-

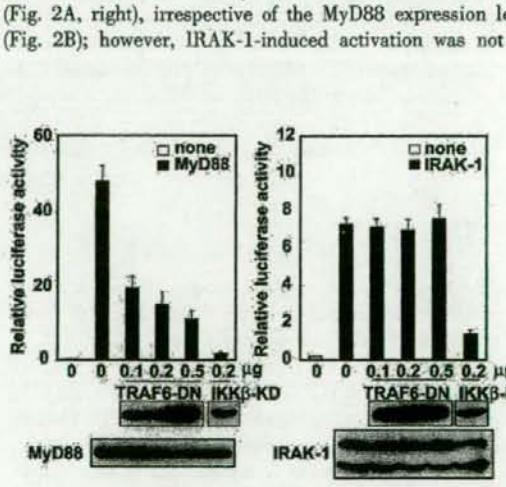


**Fig. 1.** A TRAF6 dominant-negative mutant inhibits MyD88-induced but not IRAK-1-induced activation of NF-κB. HEK293 cells were transiently transfected with a NF-κB-dependent luciferase reporter plasmid and an expression plasmid (0.1 μg) for MyD88 (left panel) or IRAK-1 (right panel) together with a kinase-dead (KD) mutant of IKKβ (K44A) or an increasing amount of a dominant-negative mutant plasmid for TRAF6 (TRAF6-DN; aa 289–522). After 30 h, cellular extracts were subjected to luciferase activity measurements and SDS-PAGE followed by immunoblotting. Values are means ± SEM from three independent experiments.

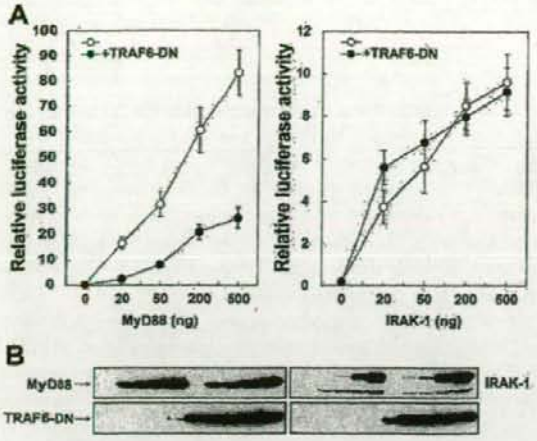


**Fig. 2.** A TRAF6 dominant-negative mutant did not affect IRAK-1-induced activation at any of the IRAK-1 expression levels. HEK293 cells were transiently transfected with a NF-κB-dependent luciferase reporter plasmid and an increasing amount of MyD88 (A) or IRAK-1 (B) expression plasmid in the absence (○) or presence (●) of a dominant-negative mutant plasmid (0.5 μg) for TRAF6 (TRAF6-DN; aa 289–522). After 30 h, cellular extracts were subjected to luciferase activity measurements and SDS-PAGE followed by immunoblotting. Values are means ± SEM from three independent experiments.

fected (Fig. 2A, left) at any of the IRAK-1 expression levels (Fig. 2B).

## MyD88-induced and IRAK-1-induced activation of NF-κB require TRAF6

Results obtained with the TRAF6 dominant-negative suggest that TRAF6 is not involved in IRAK-1-induced activation of NF-κB. To confirm this finding, the effects of a TRAF6 siRNA were examined. An increasing amount of a TRAF6 siRNA oligo was transfected into HEK293 cells with MyD88, IRAK-1, or IKKβ, and NF-κB-dependent reporter activity was measured. Unexpectedly, IRAK-1-induced (**Fig. 3B**) as well as MyD88-induced (Fig. 3A) activation of NF-κB was inhibited by the transfection of the siRNA oligo in a dose-dependent manner. IKKβ-induced activation of NF-κB was not significantly affected by the siRNA oligo (Fig. 3C), indicating that the inhibition was not nonspecific. The expression levels of MyD88, IRAK-1, and IKKβ were not affected by the TRAF6 siRNA oligo (Fig. 3, upper panels). Furthermore, another TRAF6 siRNA oligo that targets different regions of TRAF6 mRNA also inhibited MyD88 and IRAK-1-induced activation of NF-κB (data not shown). These results indicate that although IRAK-1-induced activation was not inhibited by a TRAF6 dominant-negative mutant, MyD88- and IRAK-1-induced activation of NF-κB require TRAF6.

The N-terminal region of TRAF6 is believed to be important for signal transduction. However, as IRAK-1-induced activation of NF-κB was not affected by an N-terminal deletion mutant of TRAF6 but required TRAF6, the possibility that the C-terminal portion of TRAF6 is involved in IRAK-1-induced activation of NF-κB still remains. Thus, the effect of the TRAF6 N-terminal deletion mutant was evaluated after siRNA

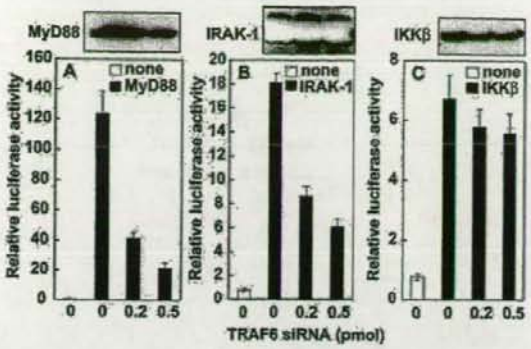


**Fig. 3.** A TRAF6 siRNA oligo inhibits MyD88-induced and IRAK-1-induced activation of NF-κB. HEK293 cells were transiently transfected with a NF-κB-dependent luciferase reporter plasmid and an expression plasmid (0.1 μg) for MyD88 (A), IRAK-1 (B), or IKKβ (C), together with an increasing amount of a TRAF6 siRNA oligo. After 30 h, cellular extracts were subjected to luciferase activity measurements and SDS-PAGE followed by immunoblotting. Values are means ± SEM from six independent experiments.

silencing of endogenous TRAF6 (**Fig. 4**). The transfection of a TRAF6 siRNA oligo did not affect basal NF-κB-dependent reporter activity. Coexpression of TRAF6, but not expression of the N-terminal deletion mutant, increased reporter activity (Fig. 4, left panel). The significant increase in reporter activity observed upon expression of MyD88 was inhibited by the transfection of the TRAF6 siRNA oligo as shown above. Under this condition, coexpression of TRAF6, but not the TRAF6 N-terminal deletion mutant, overcame the inhibition induced

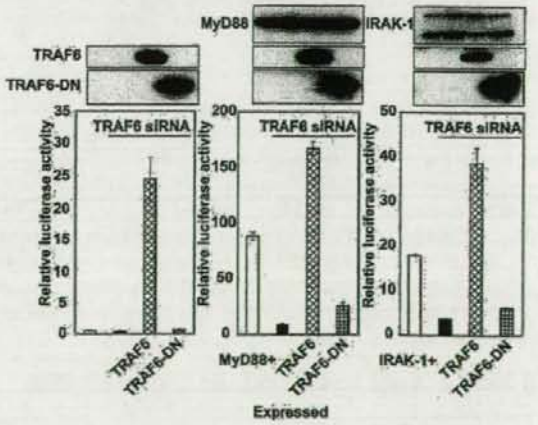


**Fig. 4.** C-terminal portion of TRAF6 is not involved in IRAK-1-induced activation of NF-κB. HEK293 cells were transiently transfected with a NF-κB-dependent luciferase reporter plasmid and a control vector (left panel), an expression plasmid (0.1 μg) for MyD88 (middle panel), or IRAK-1 (right panel) together with wild-type or a dominant-negative mutant plasmid (0.5 μg) for TRAF6 (TRAF6-DN; aa 289–522) in the absence (left bar) or presence (right three bars) of a TRAF6 siRNA oligo (0.5 pmol). After 30 h, cellular extracts were subjected to luciferase activity measurements and SDS-PAGE followed by immunoblotting. Values are means ± SEM from seven independent experiments.

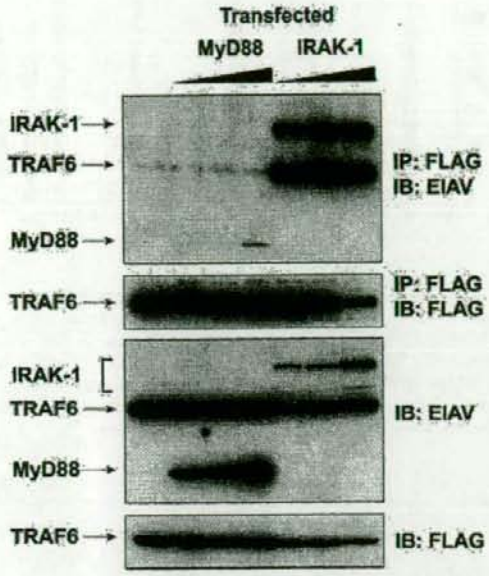


**Fig. 5.** IRAK-1 but not MyD88 induces oligomerization of TRAF6. HEK293 cells stably expressing FLAG-tagged TRAF6 and EIAV-tagged TRAF6 were transiently transfected with an expression plasmid for EIAV-tagged MyD88 or EIAV-tagged IRAK-1. After 30 h, cellular extracts were prepared, and FLAG-tagged TRAF6 was immunoprecipitated (IP). Precipitated, FLAG-tagged TRAF6 (second panel from top) and coprecipitated EIAV-tagged proteins (top panel) were detected by immunoblotting (IB). Part of each cell extract prepared above was subjected to the detection of EIAV-tagged proteins (second panel from bottom) and FLAG-tagged TRAF6 (bottom panel) by immunoblotting.

by TRAF6 siRNA (Fig. 4, middle panel). IRAK-1-induced activation of NF-κB was also inhibited by TRAF6 siRNA, and coexpression of TRAF6 again overcame the inhibition. However, coexpression of the N-terminal deletion mutant was not able to overcome the inhibition induced by TRAF6 siRNA (Fig. 4, right panel). TRAF6, the N-terminal deletion mutant of TRAF6, IRAK-1, and MyD88, was properly expressed (Fig. 4, upper panels). Thus, it is unlikely that the C-terminal portion of TRAF6 is capable of transmitting IRAK-1-induced activation of NF-κB.

## IRAK-1 but not MyD88 induces oligomerization of TRAF6

The effects of the TRAF6 N-terminal deletion mutant differed between MyD88-induced and IRAK-1-induced activation of NF-κB. The fact that TRAF6 is required for both types of activation suggests that TRAF6 is differentially involved in the activation induced by these molecules. As it has been reported that TRAF6 oligomerization induces activation of NF-κB [12, 13], the oligomerization of TRAF6 was examined in response to the expression of MyD88 and IRAK-1. HEK293 cells stably expressing FLAG-tagged TRAF6, and EIAV-tagged TRAF6 were transiently transfected with an expression plasmid for EIAV-tagged MyD88 or EIAV-tagged IRAK-1. After preparing cell extracts, FLAG-tagged TRAF6 was immunoprecipitated (**Fig. 5**, second panel from the top) with anti-FLAG M2 affinity gel, and coprecipitated, EIAV-tagged proteins were detected by immunoblotting (Fig. 5, top panel). Upon expression of MyD88, a trace amount of MyD88, but no EIAV-tagged TRAF6, was coprecipitated with FLAG-tagged TRAF6. In contrast, EIAV-tagged TRAF6 as well as IRAK-1 were coprecipitated with FLAG-tagged TRAF6 when IRAK-1 was expressed. MyD88, IRAK-1, EIAV-tagged TRAF6 (Fig. 5, second panel from the bottom), and FLAG-tagged TRAF6 (Fig. 5, bottom panel) were properly expressed. Therefore, expression of IRAK-1 but not MyD88 induces oligomerization of TRAF6.

The effect of the TRAF6 N-terminal deletion mutant on IRAK-1-induced oligomerization of TRAF6 was next examined (**Fig. 6**). HEK293 cells stably expressing FLAG-tagged TRAF6 and EIAV-tagged TRAF6 were transiently transfected with an expression plasmid for EIAV-tagged IRAK-1 and an increasing amount of a plasmid expressing the EIAV-tagged TRAF6 N-terminal deletion mutant. After preparing cell extracts, FLAG-tagged TRAF6 was immunoprecipitated (Fig. 6, right part of the top panel) with anti-FLAG M2 affinity gel, and coprecipitated, EIAV-tagged proteins were detected by immunoblotting (Fig. 6, right part of the bottom panel). Upon expression of IRAK-1, EIAV-tagged TRAF6 as well as IRAK-1 were coprecipitated with FLAG-tagged TRAF6 as shown above. When the TRAF6 N-terminal deletion mutant was coexpressed, the mutant was also precipitated with FLAG-tagged TRAF6, and the amount of coprecipitated, EIAV-tagged TRAF6 was not affected by coexpression of the TRAF6 N-terminal deletion mutant. IRAK-1, EIAV-tagged and FLAG-tagged TRAF6, and the TRAF6 deletion mutant were expressed properly (Fig. 6, left panels). Thus, the expression of the TRAF6 N-terminal deletion mutant does not appear to inhibit the IRAK-1-induced oligomerization of TRAF6. Taken together, these data demonstrate that TRAF6 is differentially

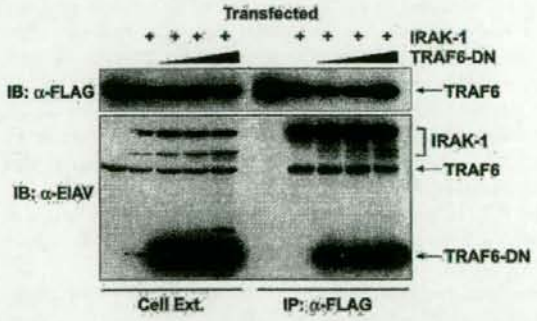


**Fig. 6.** IRAK-1 and a TRAF6 dominant-negative mutant were coprecipitated with TRAF6. HEK293 cells stably expressing FLAG-tagged TRAF6 and EIAV-tagged TRAF6 were transiently transfected with an increasing amount of a dominant-negative mutant plasmid for EIAV-tagged TRAF6 (TRAF6-DN; aa 289–522) together with an expression plasmid for EIAV-tagged MyD88 or EIAV-tagged IRAK-1. After 30 h, cellular extracts were prepared, and FLAG-tagged TRAF6 was immunoprecipitated. Precipitated, FLAG-tagged TRAF6 (right half of top panel) and coprecipitated EIAV-tagged proteins (right half of bottom panel) were detected by immunoblotting. Part of each cell extract (Cell Ext.) prepared above was subjected to the detection of EIAV-tagged proteins (left half of bottom panel) and FLAG-tagged TRAF6 (left half of top panel) by immunoblotting.

involved in MyD88-induced and IRAK-1-induced activation of NF-κB and that IRAK-1 but not MyD88 induces TRAF6 oligomerization.

## DISCUSSION

In this study, we found that TRAF6 is differentially involved in MyD88- and IRAK-1-induced activation of NF-κB. MyD88 and IRAK-1 act as adaptor molecules in TLR/IL-1R signaling, and overexpression of each molecule leads to activation of NF-κB via their downstream signaling molecule TRAF6 (see ref. [1]). These observations were confirmed in the experiment in which TRAF6 siRNAs inhibited the activation of MyD88- and IRAK-1-induced NF-κB activation (Fig. 3). However, we found that a dominant-negative mutant of TRAF6 (N-terminal deletion of aa 1–288) inhibits only MyD88-induced activation (Figs. 1 and 2). It is unlikely that IRAK-1 activates NF-κB by using the C-terminal portion of TRAF6, as IRAK-1 failed to activate NF-κB when endogenous, wild-type TRAF6 was silenced by TRAF6 siRNA, and the N-terminal deletion mutant of TRAF6 was overexpressed (Fig. 4). We also found that expression of IRAK-1 but not MyD88 leads to oligomerization of TRAF6 (Fig. 5). It has been reported that oligomerization of TRAF6 induces activation of NF-κB [12, 13]. Thus, oligomerization of TRAF6 is probably involved in the IRAK-1-induced activation of NF-κB. The N-terminal deletion mutant of TRAF6 did not inhibit IRAK-1-induced TRAF6 oligomerization. Instead, the mutant formed a complex with the TRAF6 oligomer (Fig. 6), indicating that the TRAF6 oligomer consists of more than two molecules of TRAF6. This finding explains why the N-terminal deletion mutant of TRAF6 was not able to inhibit IRAK-1-induced activation of NF-κB.

Not only does IRAK-1 induce TRAF6 oligomerization, it is also associated with the TRAF6 oligomer (Fig. 5). We found that an IRAK-1 mutant (E544A/E587A/E706A), in which three putative TRAF6-binding sites were mutated, the mutation known to greatly impair the ability to activate NF-κB [7], did not induce oligomerization of TRAF6 (data not shown), suggesting that TRAF6 molecules form a complex through the binding to IRAK-1. Overexpression of IRAK-1 in HEK293 cells appears mainly as two forms on SDS-PAGE (see Fig. 1), with the slower migrating form recognized as the hyperphosphorylated form of IRAK-1 (see ref. [1]). Interestingly, the slower migrating form of IRAK-1 was predominantly coprecipitated with the TRAF6 oligomer (see Fig. 6). It has been reported that IL-1 stimulation leads to hyperphosphorylation of IRAK-1 by autophosphorylation and to association between phosphorylated IRAK-1 and TRAF6 [4]. Thus, it is likely that autophosphorylated IRAK-1 promotes TRAF6 oligomerization by binding to TRAF6.

Overexpression of MyD88 did not induce detectable TRAF6 oligomerization (Fig. 5), although expression led to a strong activation of NF-κB (Fig. 1). TRAF6 oligomerization in response to TLR/IL-1R stimulation has not been reported. There was also no detectable TRAF6 oligomerization in cells stably expressing FLAG-tagged TRAF6 and EIAV-tagged TRAF6 in response to IL-1, LPS, or $Pam_3CSK_4$ stimulation, when these cells were transiently expressed with the IL-1RI/IL-1R accessory protein, CD14/TLR4/myeloid differentiation protein-2 or TLR1/TLR2, respectively, although these stimulations induced a strong activation of NF-κB (data not shown). Thus, it is unlikely that TRAF6 oligomerization is required for the activation of NF-κB in response to TLR/IL-1R stimulation. TRAF6 reportedly functions, in conjunction with ubiquitin-conjugating enzyme complex Ubc13-Uev1A, as a ubiquitin ligase, and this ubiquitin ligase activity is involved in the activation of NF-κB [11, 12]. We found that transfection of a Ubc13 siRNA oligo into HEK293 cells inhibited MyD88-induced activation of NF-κB (data not shown). Therefore, the ubiquitin ligase activity of TRAF6 may be involved in the MyD88-induced activation. Fukushima et al. [19] reported that LPS-induced degradation of IκBα was severely impaired in macrophages and splenocytes isolated from heterozygous $Ubc13^{+/-}$ mice. However, Yamamoto et al. [20] reported that Ubc13-deficient B cells, bone marrow macrophages, and embryonic fibroblasts showed almost normal NF-κB activation in response to LPS, IL-1β, or a bacterial lipoprotein. Thus, further studies are needed to clarify the role of the ubiquitin ligase activity of TRAF6 in TLR/IL-1R signaling.

It is considered that IRAK-1 lies downstream of MyD88 in the TLR/IL-1R signaling processes. Thus, our result that a dominant-negative mutant of TRAF6 inhibited MyD88-induced, but not IRAK-1-induced, activation of NF-κB was surprising. There are two possible explanations for this finding. One is that IRAK-1 is not necessary for TLR/IL-1R signaling. The other is that the activation of NF-κB in response to IRAK-1 overexpression is qualitatively different from the activation induced physiologically in response to TLR/IL-1R stimulation. We are not able to exclude the second possibility. However, it has been reported that macrophages from IRAK-1 knockout mice showed only partial impairment of cytokine production and NF-κB activation in response to TLR4 stimulation [21]. In addition, Kawagoe et al. [22] recently found that the IRAK-1/IRAK-4 double-knockout did not affect macrophage activator lipoprotein peptide-2-induced activation of NF-κB and proposed the existence of a TLR-mediated, IRAK-1/IRAK-4-independent signaling pathway. It is possible that another IRAK member, such as IRAK-2, compensates for the lack of IRAK-1/IRAK-4 in this knockout mouse. However, we also found that IRAK-2-induced activation of NF-κB was not inhibited by a dominant-negative mutant of TRAF6 (data not shown). Therefore, IRAK-1 may not be involved in TLR/IL-1R signaling. This possibility remains to be studied.

## ACKNOWLEDGMENTS

This research was supported in part by a grant from the Ministry of the Environment. We thank Yukiko Taguchi for technical assistance.

## REFERENCES

1. Janssens, S., Beyaert, R. (2003) Functional diversity and regulation of different interleukin-1 receptor-associated kinase (IRAK) family members. *Mol. Cell* **11**, 293–302.

2. Fujihara, M., Muroi, M., Tanamoto, K., Suzuki, T., Azuma, H., Ikeda, H. (2003) Molecular mechanisms of macrophage activation and deactivation by lipopolysaccharide: roles of the receptor complex. *Pharmacol. Ther.* **100**, 171–194.
3. Li, S., Strelow, A., Fontana, E. J., Wesche, H. (2002) IRAK-4: a novel member of the IRAK family with the properties of an IRAK-kinase. *Proc. Natl. Acad. Sci. USA* **99**, 5567–5572.
4. Cao, Z., Xiong, J., Takeuchi, M., Kurama, T., Goeddel, D. V. (1996) TRAF6 is a signal transducer for interleukin-1. *Nature* **383**, 443–446.
5. Burns, K., Janssens, S., Brissoni, B., Olivos, N., Beyaert, R., Tschopp, J. (2003) Inhibition of interleukin 1 receptor/Toll-like receptor signaling through the alternatively spliced, short form of MyD88 is due to its failure to recruit IRAK-4. *J. Exp. Med.* **197**, 263–268.
6. Muzio, M., Ni, J., Feng, P., Dixit, V. M. (1997) IRAK (Pelle) family member IRAK-2 and MyD88 as proximal mediators of IL-1 signaling. *Science* **278**, 1612–1615.
7. Ye, H., Arron, J. R., Lamothe, B., Cirilli, M., Kobayashi, T., Shevde, N. K., Segal, D., Dzivenu, O. K., Vologodskaia, M., Yim, M., Du, K., Singh, S., Pike, J. W., Darnay, B. G., Choi, Y., Wu, H. (2002) Distinct molecular mechanism for initiating TRAF6 signaling. *Nature* **418**, 443–447.
8. Li, X., Commane, M., Jiang, Z., Stark, G. R. (2001) IL-1-induced NFκB and c-Jun N-terminal kinase (JNK) activation diverge at IL-1 receptor-associated kinase (IRAK). *Proc. Natl. Acad. Sci. USA* **98**, 4461–4465.
9. Hayden, M. S., Ghosh, S. (2004) Signaling to NF-κB. *Genes Dev.* **18**, 2195–2224.
10. Chen, Z. J. (2005) Ubiquitin signaling in the NF-κB pathway. *Nat. Cell Biol.* **7**, 758–765.
11. Deng, L., Wang, C., Spencer, E., Yang, L., Braun, A., You, J., Slaughter, C., Pickart, C., Chen, Z. J. (2000) Activation of the IκB kinase complex by TRAF6 requires a dimeric ubiquitin-conjugating enzyme complex and a unique polyubiquitin chain. *Cell* **103**, 351–361.
12. Wang, C., Deng, L., Hong, M., Akkaraju, G. R., Inoue, J., Chen, Z. J. (2001) TAK1 is a ubiquitin-dependent kinase of MKK and IKK. *Nature* **412**, 346–351.
13. Baud, V., Liu, Z. G., Bennett, B., Suzuki, N., Xia, Y., Karin, M. (1999) Signaling by proinflammatory cytokines: oligomerization of TRAF2 and TRAF6 is sufficient for JNK and IKK activation and target gene induction via an amino-terminal effector domain. *Genes Dev.* **13**, 1297–1308.
14. Hirschfeld, M., Ma, Y., Weis, J. H., Vogel, S. N., Weis, J. J. (2000) Repurification of lipopolysaccharide eliminates signaling through both human and murine Toll-like receptor 2. *J. Immunol.* **165**, 618–622.
15. Sun, L., Deng, L., Ea, C. K., Xia, Z. P., Chen, Z. J. (2004) The TRAF6 ubiquitin ligase and TAK1 kinase mediate IKK activation by BCL10 and MALT1 in T lymphocytes. *Mol. Cell* **14**, 289–301.
16. Muroi, M., Ohnishi, T., Tanamoto, K. (2002) MD-2, a novel accessory molecule, is involved in species-specific actions of *Salmonella* lipid A. *Infect. Immun.* **70**, 3546–3550.
17. Muroi, M., Tanamoto, K. (2002) The polysaccharide portion plays an indispensable role in *Salmonella* lipopolysaccharide-induced activation of NF-κB through human Toll-like receptor 4. *Infect. Immun.* **70**, 6043–6047.
18. Kobayashi, N., Kadono, Y., Naito, A., Matsumoto, K., Yamamoto, T., Tanaka, S., Inoue, J. (2001) Segregation of TRAF6-mediated signaling pathways clarifies its role in osteoclastogenesis. *EMBO J.* **20**, 1271–1280.
19. Fukushima, T., Matsuzawa, S., Kress, C. L., Bruey, J. M., Krajewska, M., Lefebvre, S., Zapata, J. M., Ronai, Z., Reed, J. C. (2007) Ubiquitin-conjugating enzyme Ubc13 is a critical component of TNF receptor-associated factor (TRAF)-mediated inflammatory responses. *Proc. Natl. Acad. Sci. USA* **104**, 6371–6376.
20. Yamamoto, M., Okamoto, T., Takeda, K., Sato, S., Sanjo, H., Uematsu, S., Saitoh, T., Yamamoto, N., Sakurai, H., Ishii, K. J., Yamaoka, S., Kawai, T., Matsuura, Y., Takeuchi, O., Akira, S. (2006) Key function for the Ubc13 E2 ubiquitin-conjugating enzyme in immune receptor signaling. *Nat. Immunol.* **7**, 962–970.
21. Swantek, J. L., Tsen, M. F., Cobb, M. H., Thomas, J. A. (2000) IL-1 receptor-associated kinase modulates host responsiveness to endotoxin. *J. Immunol.* **164**, 4301–4306.
22. Kawagoe, T., Sato, S., Jung, A., Yamamoto, M., Matsui, K., Kato, H., Uematsu, S., Takeuchi, O., Akira, S. (2007) Essential role of IRAK-4 protein and its kinase activity in Toll-like receptor-mediated immune responses but not in TCR signaling. *J. Exp. Med.* **204**, 1013–1024.

*Oral Microbiology Immunology 2008: 23: 60–69*
*Printed in Singapore. All rights reserved*



ORAL MICROBIOLOGY
AND IMMUNOLOGY

# Biological properties of the native and synthetic lipid A of *Porphyromonas gingivalis* lipopolysaccharide

**H. Kumada[1], Y. Haishima[2], K. Watanabe[1], C. Hasegawa[2], T. Tsuchiya[2], K. Tanamoto[3], T. Umemoto[1]**
[1]Department of Oral Microbiology, Kanagawa Dental College, Yokosuka, Kanagawa, Japan, [2]Divisions of Medical Devices, National Institute of Health Sciences, Setagaya, Tokyo, Japan, [3]Divisions of Microbiology, National Institute of Health Sciences, Setagaya, Tokyo, Japan

*Kumada H, Haishima Y, Watanabe K, Hasegawa C, Tsuchiya T, Tanamoto K, Umemoto T. Biological properties of the native and synthetic lipid A of* Porphyromonas gingivalis *lipopolysaccharide.*
*Oral Microbiol Immunol 2008: 23: 60–69.* © 2008 The Authors. Journal compilation © 2008 Blackwell Munksgaard.

**Introduction and methods:** A pentaacyl and diphosphoryl lipid A molecule found in the lipid A isolated from *Porphyromonas gingivalis* lipopolysaccharide (LPS) was chemically synthesized, and its characteristics were evaluated to reconfirm its interesting bioactivities including low endotoxicity and activity against LPS-unresponsive C3H/HeJ mouse cells.
**Results:** The synthesized *P. gingivalis* lipid A (synthetic Pg-LA) exhibited strong activities almost equivalent to those of *Escherichia coli*-type synthetic lipid A (compound 506) in all assays on LPS-responsive mice, and cells. LPS and native lipid A of *P. gingivalis* displayed overall endotoxic activities, but its potency was reduced in comparison to the synthetic analogs. In the assays using C3H/HeJ mouse cells, the LPS and native lipid A significantly stimulated splenocytes to cause mitosis, and peritoneal macrophages to induce tumor necrosis factor-α and interleukin-6 production. However, synthetic Pg-LA and compound 506 showed no activity on the LPS-unresponsive cells. Inhibition assays using some inhibitors including anti-human Toll-like receptor 2 (TLR2) and TLR4/MD-2 complex monoclonal antibodies showed that the biological activity of synthetic Pg-LA was mediated only through the TLR4 signaling pathway, which might act as a receptor for LPS, whereas TLR2, possibly together with CD14, was associated with the signaling cascade for LPS and native lipid A of *P. gingivalis*, in addition to the TLR4 pathway.
**Conclusion:** These results suggested that the moderated and reduced biological activity of *P. gingivalis* LPS and native lipid A, including their activity on C3H/HeJ mouse cells via the TLR2-mediated pathway, may be mediated by bioactive contaminants or low acylated molecules present in the native preparations having multiple lipid A moieties.

Key words: biological properties; lipopolysaccharide; *Porphyromonas gingivalis;* synthetic lipid A

Hidefumi Kumada, Department of Oral Microbiology, Kanagawa Dental College, 82 Inaoka-cho, Yokosuka, Kanagawa 238-8580, Japan
Tel./fax: +81 46 822 8867;
e-mail: kumadahi@kdcnet.ac.jp
Accepted for publication April 6, 2007

*Porphyromonas gingivalis*, an oral anaerobic gram-negative rod, is thought to be the most important mediator of the pathogenicity of periodontal disease (15, 47, 60). Many investigations have shown that the lipopolysaccharide (LPS) of *P. gingivalis* is a significant virulence factor, because it exhibits various activities, such as induction of inflammatory cytokines in human gingival fibroblast (HGF) cultures (12, 51) and bone resorption activity (18, 32), that are closely correlated with periodontal disease. *Porphyromonas gingivalis* LPS expresses a low level of endotoxic activity relative to enterobacterial LPS (29, 32). In addition, the LPS characteristically stimulates the splenocytes and macrophages from LPS-unresponsive C3H/HeJ mice

to cause mitosis or cytokine induction (8, 24, 59), in contrast to usual LPS, which do not exhibit any effects on these cells (43, 46).

The pathophysiological activity of LPS is dependent on the chemical structure of the hydrophobic portion, called lipid A, the biologically active center of LPS (16, 42). Recently, we found a characteristic structure of *P. gingivalis* lipid A containing branched and relatively longer fatty acids (15–17 carbon atoms) that are not present in enterobacterial lipid A molecules (26). In addition, we demonstrated, using LPS-antagonist and well-purified lipid A (although containing a small amount of protein), that the characteristic action of *P. gingivalis* lipid A against C3H/HeJ mice seems to be specifically mediated by the lipid A portion (54). These results suggested that the unique fatty acid components might be associated with the activity on C3H/HeJ mouse cells. This was also supported by studies of the chemical and biological properties of *Flavobacterium meningosepticum* lipid A, which has a structure very similar to *P. gingivalis* lipid A and also activates C3H/HeJ mouse cells (21, 56).

Toll, a *Drosophila* receptor molecule with extracellular leucine-rich repeats that currently has 10 published members [Toll-like receptors (TLRs) 1–10] in humans, has a role in triggering innate defenses against bacteria or fungi (1, 30, 52). Recent studies have suggested that TLR4, a member of the TLR family, might act as a receptor for LPS (4, 17, 39). TLR4 alone is not capable of sensing and signaling the presence of LPS, but another accessory molecule, MD-2, which is physically associated with TLR4, is required for LPS recognition through TLR4 (45). On the other hand, TLR2 has been proposed as a receptor for many microbial products and has been shown to signal the presence of peptidogylcan, lipoteichoic acid, lipoarabinomannan, lipoproteins and lipopeptides, as well as many whole gram-positive bacteria (4, 53). In addition, it has been reported that the co-dominant $LPS^d$ allele of C3H/HeJ mice corresponds to a missense mutation in the third exon of the *TLR4* gene, which is predicted to result in replacement of proline with histidine at position 712 of the protein (39). Recently, we found that HGFs constitutively express *TLR2* and *TLR4*, and that their levels of expression are increased by stimulation with *P. gingivalis* LPS (50). These observations suggest that, in addition to TLR4, the biological action of *P. gingivalis* LPS may be mediated through the TLR2 pathway, which might not be correlated with LPS-mediated signaling.

In the present study, we chemically synthesized a pentaacyl and diphosphoryl lipid A analog corresponding to the lipid A species with the highest molecular mass found in *P. gingivalis* native lipid A in our previous study (26). The synthetic analog was subjected to biological assay to evaluate whether the interesting activity of LPS against C3H/HeJ mice is derived from the lipid A part.

## Materials and methods

### Reagents

RNase A, DNase I, and proteinase K were purchased from Sigma (St Louis, MO). (*R,S*)-3-hydroxy-13-methyltetradecanoic acid (3-OH-$iC_{15:0}$), (*R,S*)-3-hydroxy-15-methylhexadecanoic acid (3-OH-$iC_{17:0}$) and (*R,S*)-3-hydroxyhexadecanoic acid (3-OH-$C_{16:0}$) were purchased from Iatron-Biosupply Co. (Tokyo, Japan) and Wako Chemical Co. (Osaka, Japan). Quantitative *Limulus* amebocyte lysate (LAL) gelation assay reagent, Endospecy, was obtained from Seikagaku Kogyo (Tokyo, Japan). Iscove's modified Dulbecco and RPMI-1640 media were the obtained from Life Technologies (Grand Island, NY) and Gibco Laboratories (Grand Island, NY). [$^3$H]Thymidine was obtained from New England Nuclear (Boston, MA). Mono-Mac-6 (MM6) cells were purchased from the German Collection of Microorganisms and Cell Cultures (Braunschweig, Germany). HTA125, TL2.1, and MY4 clones, monoclonal antibodies (mAbs) to the human TLR4/MD-2 complex, and human TLR2 and CD14 molecules were purchased from MBL Medical & Biological Laboratories Co. (Nagoya, Japan), Cascade BioScience, (Winchester, MA) and Coulter Co. (Miami, FL), respectively.

### Microbes

*P. gingivalis* SU63, isolated from a periodontal pocket, was grown anaerobically at 37°C for 24 h in heart infusion broth (Difco Laboratories, Detroit, MI) supplemented with 0.0005% hemin, 0.0001% vitamin K1, 0.5% yeast extract, and 0.08% cysteine (25). The cells were heated (121°C for 15 min), harvested by centrifugation (7000 ***g***, 20 min), and washed successively with distilled water and acetone.

### Animals

Japanese White rabbits were purchased from Japan SLC, Inc. (Hamamatsu, Japan). Female C3H/HeN and C3H/HeJ mice aged 6 weeks were obtained from Clea Japan, Inc. (Tokyo, Japan), and used for the assay of splenic mitogenicity and the induction of tumor necrosis factor-α (TNF-α) and interleukin-6 (IL-6) by peritoneal macrophages.

### Preparations of *P. gingivalis* LPS and lipid A

The procedures for the preparation of *P. gingivalis* LPS and lipid A were described previously (26). Briefly, the LPS was extracted from acetone-dried cells with phenol–water (58), digested with RNase A, DNase I, and proteinase K (44), and then purified by repeated ultracentrifugation (105,000 ***g***, 12 h, six times). The LPS was washed successively with phenol/chloroform/petroleum ether [2 : 5 : 8, volume/volume (V/V)] (10) and acetone and then lyophilized.

The free lipid A was recovered from hydrolysates (1% acetic acids, 100°C, 1.5 h) of LPS according to the methods of Qureshi et al. (40, 41). It was purified by passage through a Dowex 50 ($H^+$) column with chloroform/methanol (3 : 1, V/V) as the eluent and gel permeation chromatography with a Sephadex LH-20 (Pharmacia, Uppsala, Sweden) column with the same solvent as the eluent (26).

### Total synthesis of *P. gingivalis* SU63 lipid A

*P. gingivalis* lipid A analog (compound 1) (Fig. 1) was synthesized basically according to the procedure previously reported (26). As shown in Fig. 2, (*R,S*)-3-OH-$iC_{15:0}$, (*R,S*)-3-OH-$iC_{17:0}$ and (*R,S*)-3-OH-$C_{16:0}$ were selectively (*S*)-3-*O*-acetylated by lipase treatment (5) of the methyl esters. The non-acetylated methyl esters predominantly containing the (*R*)-forms were separated by silica-gel chromatography, and each free acid was fractionally crystallized from $CH_3CN$ as the dibenzylamine salt to increase the percentage of enantiomorphic excess. The optically pure (*R*)-3-OH fatty acids (compounds 2–4) were converted to the phenacyl ester (compounds 5–7) and 3-*O*-acylated with $C_{16:0}$ or benzyloxycarbonyl chloride (Z-Cl) to obtain the phenacyl ester of (*R*)-3-*O*-Z-$iC_{15:0}$ (compound 8), (*R*)-3-*O*-Z-$C_{16:0}$ (compound 9), (*R*)-3-*O*-Z-$iC_{17:0}$ (coumpound 10) and (*R*)-3-*O*-(hexadecanoyl)-15-methylhexadecanoic acid [3-*O*-($C_{16:0}$)-$iC_{17:0}$] (compound 11). After dephenacylation, each fatty acid (compounds 12–15) was purified by silica-gel chromatography, and the yields of

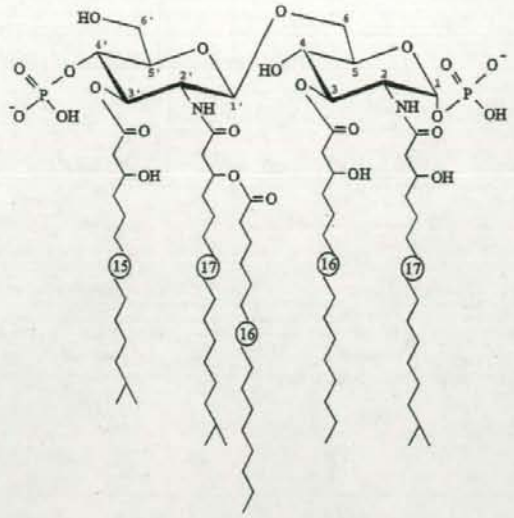

*Fig. 1.* Chemical structure of *Porphyromonas gingivalis* synthetic lipid A. In this study, we chemically synthesized a pentaacyl and diphosphoryl lipid A analog corresponding to the lipid A species with the highest molecular mass found in *P. gingivalis* native lipid A in our previous study (26). The synthetic Pg-LA consists of β(1-6)-linked D-glucosamine disaccharide 1,4'-bisphosphate backbone acylated with (*R*)-3-OH-$iC_{17:0}$, (*R*)-3-OH-$C_{16:0}$, (*R*)-3-OH-($C_{16:0}$)-$iC_{17:0}$ and (*R*)-3-OH-$iC_{15:0}$ at positions 2, 3, 2' and 3' of the hydrophilic backbone.

compounds 12–14 were 8.9%, 24.1%, and 9.7%, respectively.

The glycosyl donors were prepared from *N*-(2,2,2-trichloroethoxycarbonyl)-D-glucosamine (compound 16) as shown in FIG. 3. After allyl glycosidation, isopropylidenation of the glycoside followed by simple recrystallization afforded almost pure 4,6-*O*-isopropylidenated α-allyl glycoside, compound 17. This product was 3-*O*-acylated with (*R*)-3-*O*-Z-$iC_{15:0}$ to obtain compound 18, and the 4,6-*O*-protection was removed by mild acid hydrolysis to give product 19. Position 6 of the compound was protected with a carbobenzoxyl group to synthesize compound 20 followed by 4-*O*-diphenylphosphorylation (compound 21) and subsequent cleavage of the allyl group to make compound 22 (33, 38). This product was allowed to react with $CCl_3CN$ in the presence of $Cs_2CO_3$ (57) as a catalyst to give glycosyl trichloroacetimidate, compound 23, to be used as the donor.

On the other hand, glycosyl acceptor was prepared through compound 17 (Fig. 4). The compound was 3-*O*-acylated with (*R*)-3-*O*-Z-$C_{16:0}$ to obtain compound 24. After removing the Troc group, the product 25 was *N*-acylated with (*R*)-3-*O*-Z-$iC_{17:0}$ to give compound 26 followed by cleavage of the 4,6-*O*-protection to yield glycosyl acceptor 27. Coupling reaction of compound 23 with 27 was performed using trimethylsilyl triflate (TMSOTf) in 1,2-dichloroethane to obtain disaccharide 28, which gave the desired β(1 → 6) linkage in a higher yield than the Kŏnigs–Knorr and oxazoline methods (9, 19). After removing the Troc group of the disaccharide compound, the 2'-amino group of product 29 was *N*-acylated with (*R*)-3-*O*-($C_{16:0}$)-$iC_{17:0}$ to prepare compound 30. Compound 31 with a free 1-hydroxyl group was prepared by cleavage of the allyl group, and then 1α-*O*-phosphorylation to yield the protected 1,4'-bisphosphate compound 32 was performed by 1-*O*-lithiation with buthyllithium (BuLi) and subsequent treatment with tetrabenzyl diphosphate (9, 19, 20). The product purified using silica-gel chromatography was deprotected by two-step hydrogenolysis (8 kg/cm$^2$ of $H_2$) with Pd-black in THF and subsequent platinum

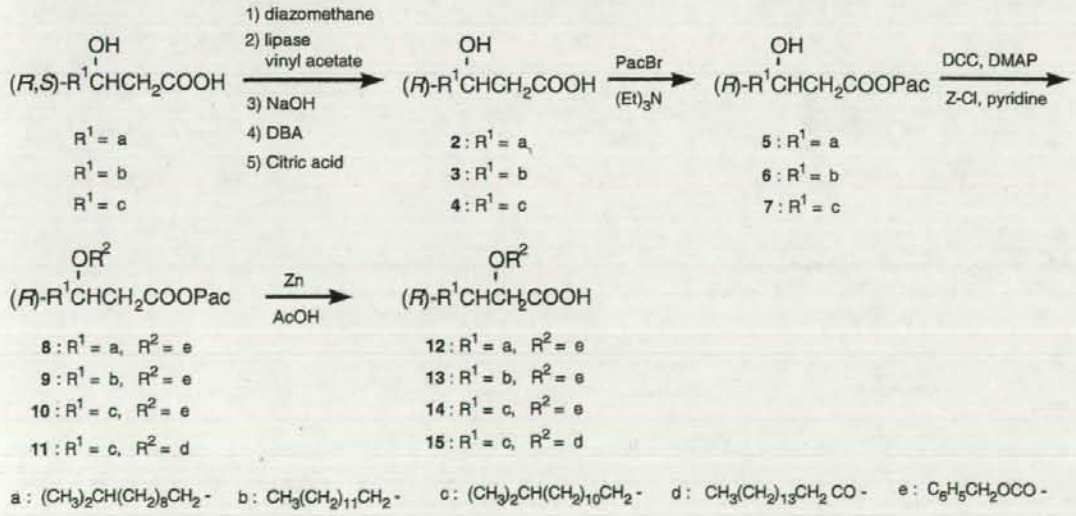


*Fig. 2.* Synthesis of (*R*)-3-hydroxy fatty acids; (*R*)-3-OH-$iC_{15:0}$, (*R*)-3-OH-$C_{16:0}$, (*R*)-3-OH-$iC_{17:0}$ and (*R*)-3-OH-($C_{16:0}$)-$iC_{17:0}$. Synthetic procedures of each fatty acid are described in the Materials and methods.

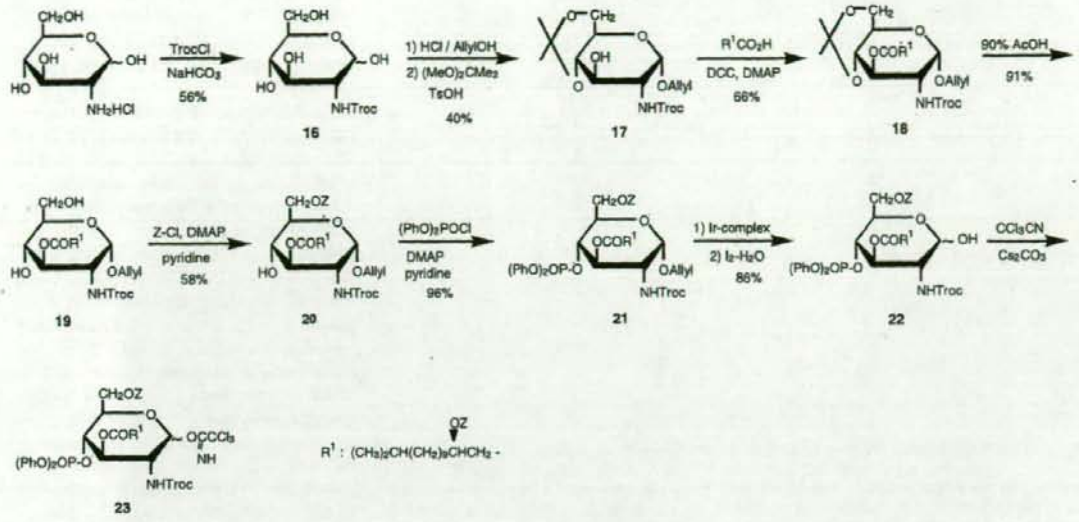

*Fig. 3.* Total synthesis of *Porphyromonas gingivalis* lipid A (step 1). Step 1 was performed for the preparation of a glycosyl donor corresponding to the terminal residue. Synthetic procedures of step 1 are described in the Materials and methods.

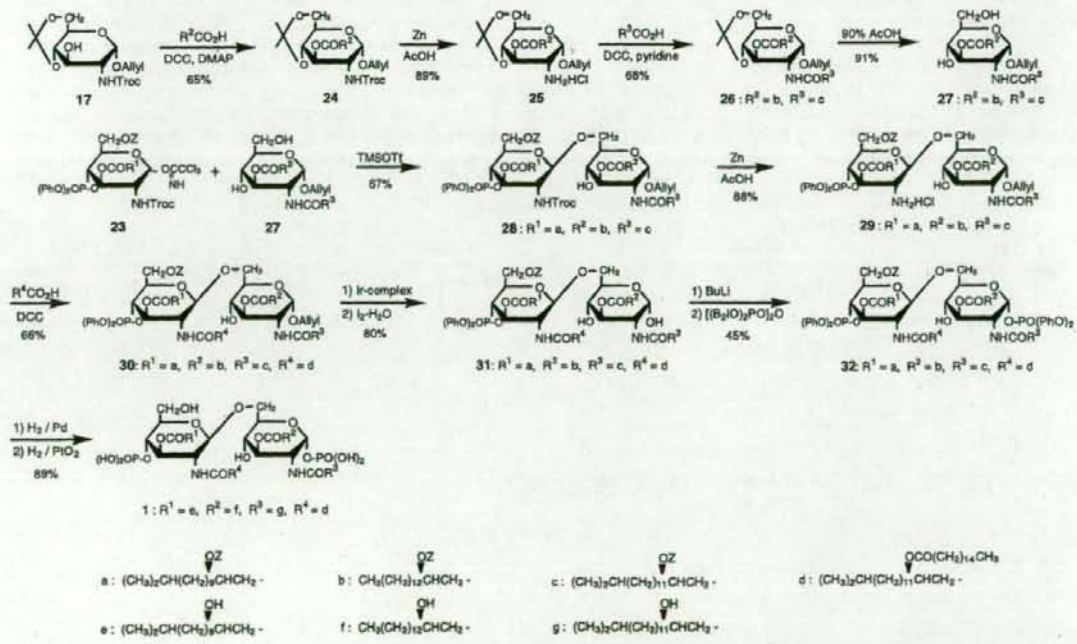

*Fig. 4.* Total synthesis of *Porphyromonas gingivalis* lipid A (step 2). Step 2 involved the preparation of a glycosyl acceptor corresponding to a non-terminal residue and coupling reaction of each unit. Synthetic procedures of step 2 are described in the Materials and methods.

oxide ($PtO_2$) in THF-$H_2O$ (20 : 1) to give a good yield of *P. gingivalis* lipid A analog (compound 1), synthetic *P. gingivalis* lipid A (Pg-LA). Finally, the analog was effectively purified by centrifugal partition chromatography (49) using $CHCl_3$-MeOH-iPrOH-$H_2O$-$Et_3N$ = 20 : 20 : 2.5 : 22.5 : 0.01 as a two-phase eluate on a Model LLB-M instrument (Sanki Engineering Ltd., Kyoto, Japan). The structure was confirmed by liquid secondary ion-mass spectrometry (m/z 1768.2 $[M-H]^-$) in negative ion mode and by nuclear magnetic resonance spectroscopy, which demonstrated

β-configuration of the glycosidic linkage, linkage positions of phosphate groups (1 and 4'), and α-configuration of the phosphorylated position 1.

#### Liquid secondary ion-mass spectrometry and nuclear magnetic resonance spectroscopy

Both liquid secondary ion-mass spectrometry and nuclear magnetic resonance spectroscopy were performed according to the methods reported previously (26).

#### LAL gelation assay

LAL gelation activity was measured by the chromogenic endotoxin-specific assay, Endospecy, using recombinant *Limulus* coagulation enzyme from horseshoe crab (34). Aliquots of 50-μl samples were incubated with the same volume of lysate containing chromogenic substrate in 96-well flat microplates at 37°C for 30 min. The absorbance was measured with a microplate reader (Wellreader SK-601, Seikagaku Kogyo) at 405 and 492 nm simultaneously, the latter as a reference. The data were expressed as the Δ absorbance (405–492 nm) per minute [ΔAbs/min (405–492 nm)].

#### Schwartzman assay

As described previously (27), the dermal Schwartzman assay was performed by injecting three male Japanese White rabbits (1.5–2.0 kg) intradermally into the shaved abdomen with 1, 10, or 100 μg of samples in 0.1 ml Dulbecco's phosphate buffered saline (PBS) (Nissui Pharmaceutical Co., Tokyo, Japan), followed 24 h later by a challenge intravenous injection of 100 μg *Salmonella typhimurium* LPS (Sigma) in 0.1 ml Dulbecco's PBS. The injection sites were examined for hemorrhagic necrosis 5 h after injection of the challenge dose. The results were expressed as the minimum dose of each sample to cause a hemorrhagic necrosis spot over 0.5 mm in diameter at the injection site.

#### Mitogenicity assay

Mitogenic activity was examined by the incorporation of [$^3$H]thymidine into spleen cells from C3H/HeN and C3H/HeJ mice as described (54). Mouse spleen cells were suspended in serum-free Iscove's modified Dulbecco's medium and washed with the same medium. The cells ($8 \times 10^5$ cells/0.2 ml/well) were cultured in 96-well microplates containing various amounts of samples for 72 h at 37°C in a humidified 5% $CO_2$ atmosphere. During the final 24 h, 0.5 mCi (18.5 kBq) of [$^3$H]thymidine (18.2 Ci/mmol) per well was added and the incorporation of [$^3$H]thymidine by the cultured cells was measured with a liquid scintillation counter. The results were expressed as mean counts per minute (c.p.m.) of triplicate determinations.

#### Stimulation of murine macrophages and HGFs

Mouse peritoneal macrophages were obtained from C3H/HeN and C3H/HeJ mice injected intraperitoneally with 3.0 ml thioglycollate medium. The peritoneal cells ($1 \times 10^6$ cells/ml), suspended in serum-free RPMI medium, were incubated for 2 h at 37°C in a humidified 5% $CO_2$ atmosphere. After incubation, adherent cells were stimulated for 47 h with samples to induce TNF-α and IL-6 production, and then the cell-free supernatants, passed through 0.22-μm Millex filters (Millipore Co., Bedford, MA), were stored at –20°C until used for the assays.

Normal HGFs obtained from patients were established by the explant growth method from clinically healthy gingival tissues as described elsewhere (61). The HGFs from passage 5 to 12 were cultured in Dulbecco's modified Eagle's medium (Nissui Pharmaceutical Co.) containing 10% fetal calf serum (Gibco), penicillin (100 U/ml), and streptomycin (100 μg/ml) under 5% $CO_2$. After incubation for 4 days, the fibroblast layers were washed twice with Dulbecco's modified Eagle's medium and then incubated with 1 μg/ml of each sample without fetal calf serum for 47 h. The cell-free supernatants were harvested and stored at –20°C until used for the assays.

#### Cytokine assays

TNF-α and IL-6 activity in murine–macrophage culture supernatants were determined in duplicate using an enzyme-linked immunosorbent assay (ELISA) kit (Genzyme Co., Cambridge, MA), respectively.

TNF-α production was assayed using clone MM6-CA8 derived from Mono-Mac-6 (MM6) cells, a human monocytoid cell line with high sensitivity to LPS stimulation (48). MM6-CA8 cells exhibit a superior response to low concentrations of endotoxin and peptidogylcan in producing proinflammatory cytokines. MM6-CA8 cells were cultured in RPMI-1640 medium containing fetal bovine serum (10%), glutamine (2 mM), non-essential amino acids (0.1 mM), sodium pyruvate (1 mM) and bovine insulin (9 μg/ml). After cell priming (72 h) with calcitriol (1,25-dihydroxy-vitamin D3), the cells ($1 \times 10^6$ cells ; 0.9 ml/well) were seeded in 24-well plates, and various dilutions (0.1 ml) of sample were added. After incubation for 17 h, TNF-α released into the culture supernatants was immunoenzymatically measured using commercial ELISA kits as described above.

#### Inhibition assays

To examine the effects of polymyxin B and mAb to CD14 on the production of IL-8, 100 U/ml of polymyxin B sulfate (Sigma) and 2.5 μg/ml anti-CD14 (MY4, Coulter Co., Miami, FL) was added simultaneously or after pretreatment for 2 h, respectively, to the HGF cultures stimulated with 1 μg/ml of samples for 47 h. The production of IL-8 from HGFs was determined in duplicate using a human IL-8 ELISA kit (Amersham, Piscataway, NJ).

For the inhibition assay of TNF-α from MM6-CA8 cells, 5 μg/ml anti-human TLR2 and TLR4/MD-2 complex mAbs, and 10 μg/ml anti-human CD14 were added to MM6-CA8 cell suspension in 24-well plates, and after 1 h, each sample (10 ng/ml native lipid A, and 1 ng/ml synthetic Pg-LA and 506) was added to the cell suspension. After incubation, TNF-α production by the cells was measured.

## Results

#### LAL gelation activity

The LAL gelation activity of each sample was estimated by the kinetic-chromogenic assay using LPS-specific reagent. As shown in Fig. 5, the activity increased in a dose-dependent manner over the range of concentrations tested (1 pg/ml to 1 μg/ml). Synthetic Pg-LA exhibited strong LAL gelation activity equivalent to that of compound 506, which was used as a control. On the other hand, LAL activities of *P. gingivalis* LPS and native lipid A, reported previously as a weakly toxic endotoxin (55), were approximately 10,000-fold or 100-fold weaker than that of compound 506, respectively.

#### Schwartzman reaction

Localized Schwartzman activity in rabbits was measured, and the results are shown in Table 1. *S. typhimurium* LPS and compound 506, used as positive controls, exhibited strong activity, and the minimum doses to induce a Schwartzman reaction of

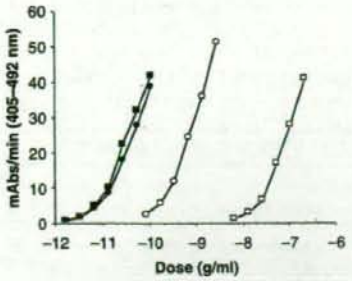


*Fig. 5.* LAL gelation activity of *Porphyromonas gingivalis* synthetic lipid A. LAL gelation activity was estimated by the kinetic-chromogenic assay using the LPS-specific reagent, Endospecy. Fifty-microliter aliquots of samples were incubated with the same volume of lysate at 37°C for 30 min. The data are expressed as the Δ absorbance (405–492 nm) per minute [ΔAbs/min (405–492 nm)]. ●, synthetic Pg-LA; ○, native lipid A; □, LPS; ■, compound 506.

each sample were 5 and 10 μg/site, respectively. Schwartzman activity of synthetic Pg-LA was similar to that of these positive controls, and the minimum inducing dose was 10 μg/site. However, minimum inducing doses of *P. gingivalis* LPS and native lipid A were 100 and 50 μg/site, respectively.

### Mitogenicity

The mitogenic activities of samples were tested on murine splenic cells from LPS-responsive C3H/HeN and LPS-unresponsive C3H/HeJ mice. As shown in Fig. 6A, synthetic Pg-LA and compound 506 showed activity in response to splenic cells from C3H/HeN mice even at a dose of 1 μg/ml, and the activity increased in a dose-dependent manner over the dose range tested. *P. gingivalis* native lipid A also exhibited activity similar to those of both synthetic compounds. As shown in Fig. 6B, significant mitogenicity was observed in the splenic cells from LPS-unresponsive C3H/HeJ mice treated with

*Table 1.* Minimum dose of *Porphyromonas gingivalis* synthetic lipid A inducing a local Schwartzman reaction

| Stimulants | Minimum inducing dose (μg/site) |
|---|---|
| *P. gingivalis* | |
| synthetic lipid A | 10 |
| native lipid A | 50 |
| LPS | 100 |
| Compound 506 | |
| *S. typhimurium* | 5 |

The minimum dose of samples for positive reaction was determined as the amount inducing a hemorrhagic spot more than 0.5 mm in diameter.

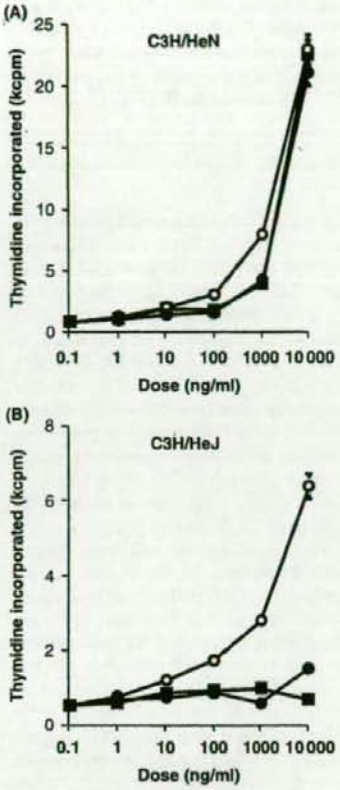


*Fig. 6.* Mitogenic responses of murine spleen cells from C3H/HeN and C3H/HeJ mice to *Porphyromonas gingivalis* synthetic lipid A. Spleen cells ($8 \times 10^5$ cells/0.2 ml) were cultured in 96-well microplates containing various amounts of samples for 72 h. During the final 24 h, 0.5 mCi (18.5 kBq) of [$^3$H]thymidine (18.2 Ci/mmol) per well was added. The results are expressed as mean c.p.m. ± SD of triplicate experiments. ●, synthetic Pg-LA; ○, native lipid A; ■, compound 506.

*P. gingivalis* native lipid A, whereas synthetic Pg-LA and control compound 506 had no mitogenic activity even at a concentration of 10 μg/ml.

### Induction of inflammatory cytokine release from various cells

Cytokine production by lipid A stimulation was assayed using HGFs, peritoneal macrophages from C3H/HeN and C3H/HeJ mice, and human MM6-CA8 cells. As shown in Table 2, native lipid A and synthetic Pg-LA exhibited activity for IL-8 induction activity in HGFs that was similar to that of compound 506 (1132.6, 1085 and 1056.9 pg/ml, respectively). The activity of synthetic analogs was significantly inhibited by polymyxin B and anti-CD14 mAb, whereas that of native lipid A was not inhibited by polymyxin B and anti-human CD14 mAb reduced the activity by only 50%.

Synthetic compound 506, used as a control, exhibited strong TNF-α and IL-6 induction in thioglycollate-elicited peritoneal macrophages from LPS-responsive C3H/HeN mice at doses of <10 ng/ml, as shown in Figs 7A and 8A. The activities of *P. gingivalis* synthetic and native lipid A were approximately 10- to 100-fold weaker than those of compound 506, respectively (Figs 7A and 8A). The *P. gingivalis* native lipid A significantly stimulated TNF-α and IL-6 production in peritoneal macrophages from LPS-unresponsive C3H/HeJ mice (Figs 7B and 8B). These LPS-unresponsive mice showed a similar minimum lipid A stimulatory dose and similar levels of cytokine production to C3H/HeN mice (Figs 7A and 8A). However, no induction of TNF-α or IL-6 release was observed with synthetic Pg-LA and compound 506, as shown in Figs 7B and 8B.

As shown in Table 3, synthetic Pg-LA and compound 506 stimulated TNF-α production in human monocytoid MM6-CA8 cells even at a low dose (each 1 ng/ml), whereas moderate activity in the cells was observed by native lipid A (10 ng/ml). Anti-human TLR4/MD-2 complex mAb significantly blocked the TNF-α production by synthetic Pg-LA and compound 506, whereas 7% inhibition and 6% inhibition were observed by anti-human TLR2 mAb (Table 3). On the other hand, both anti-human TLR2 and TLR4/MD-2 complex mAbs were essential to suppress cytokine production by *P. gingivalis* native lipid A (Table 3). In addition, anti-human CD14 mAb also completely inhibited TNF-α production induced by synthetic Pg-LA and compound 506, but approximately 70% inhibition was observed by native lipid A, as well as the results of the IL-8 production from HGF cells (Table 2).

## Discussion

In the present study, we synthesized an analog of *P. gingivalis* lipid A according to the chemical structure proposed in our previous report (26), to reconfirm the biological data reported to date by some investigators using LPS or native lipid A (8, 24, 50, 54, 55, 59), including its action on C3H/HeJ mice. Some reports suggested that *P. gingivalis* LPS possesses lipid A structural heterogeneity, consisting of only a tri-acylated monophosphorylated form (37), and of a multiple heterogeneity

*Table 2.* Effects of anti-CD14 mAb on the production of IL-8 from human gingival fibroblasts stimulated with *Porphyromonas gingivalis* synthetic lipid A

| | IL-8-producing activity | | |
|---|---|---|---|
| | | Treatment | |
| Stimulants | | Polymyxin B | Anti-CD14 |
| *P. gingivalis* | | | |
| synthetic lipid A | 1085.0 ± 15.2 | 12.5 ± < 0.1 | 301.3 ± <0.1 |
| native lipid A | 1132.6 ± 2.9 | 1251.8 ± 80.5 | 640.8 ± 33.6 |
| Compound 506 | 1056.9 ± 21.1 | 9.9 ± < 0.1 | 118.9 ± 14.1 |
| None | 12.2 ± <0.1 | 1.5 ± < 0.1 | 2.2 ± < 0.1 |

Human gingival fibroblasts were cultured with 1 μg/ml of each sample for 48 h. Polymyxin B (100 U/ml) was added simultaneously with stimulant cultivation and anti-CD14 mAb MY4 (2.5 mg/ml) was precultured for 2 h.

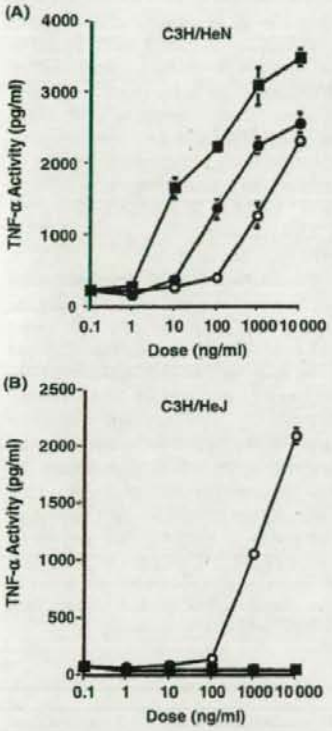


*Fig. 7.* Induction of TNF-α release from murine peritoneal macrophages from C3H/HeN and C3H/HeJ mice stimulated by *Porphyromonas gingivalis* synthetic lipid A. Thioglycollate-induced peritoneal macrophages ($1 \times 10^6$ cells/ml), suspended in serum-free RPMI medium, were incubated for 2 h. After incubation, cells were stimulated for 47 h with various amounts of samples, and then the supernatants were examined for TNF-α. The results are expressed as means ± SD of duplicate experiments. ●, synthetic Pg-LA; ○, native lipid A; ■, compound 506.

regarding the degree of acylation and/or phosphorylation; tetra- and penta-acylated monophosphorylated species seem to be the predominant molecules (3, 7, 26). In particular, Darveau's group and others have reported that specific bacteria, such as *P. gingivalis*, *Yersinia pestis*, and *S. typhimurium*, possess the ability to alter or regulate these lipid A forms under specific environmental conditions, and these lipid A alterations might modify the innate host responses to each pathogenic bacterium (3, 6, 7, 11, 22). However, these lipid A species may not reflect the complete structure of *P. gingivalis* lipid A, because pentaacyl and diphosphoryl molecules were detected in the native lipid A complexes, although this is not the main species of *P. gingivalis* lipid A (26). The analog synthesized in this study consisted of a β(1–6)-linked D-glucosamine disaccharide 1,4′-bisphosphate backbone acylated with (*R*)-3-hydroxy-15-methylhexadecanoic acid, (*R*)-3-hydroxyhexadecanoic acid, (*R*)-3-*O*-(hexadecanoyl)-15-methylhexadecanoic acid and (*R*)-3-hydroxy-13-methyltetradecanoic acid at positions 2, 3, 2′, and 3′ of a hydrophilic backbone, as shown in Fig. 1. This analog represents a lipid A molecule with the highest molecular mass of all the species found in native lipid A complexes (26), and does not contain bioactive contaminants including the LPS protein (54) or lipopeptide (13, 28) that is present in native preparations. Nor does it have the heterogeneity that may lead to decreased endotoxicity based on the elimination of acyl and phosphoryl groups in the native lipid A complex (55), eliciting low endotoxic activities of synthetic *P. gingivalis* lipid A (compound PG-381), which consists of triacylated monophosphorylated lipid A molecule (35–37).

The endotoxic activities of *P. gingivalis* LPS or native lipid A were moderate relative to that of compound 506, which was used as a control, and significantly stimulated cells from LPS-unresponsive C3H/HeJ mice, as reported previously (8, 24, 54, 55, 59). However, *P. gingivalis* synthetic lipid A exhibited an activity similar to that of compound 506 in all the biological assays in this study, including the test using LPS-unresponsive C3H/HeJ mice. These results indicated that fully acylated and phosphorylated *P. gingivalis* lipid A is a strong agonist and, at the least, low toxicity and biological activity against LPS-unresponsive mice found in the LPS may not be dependent on the unique acyl residues, iso-form fatty acids consisting of 15–17 carbon atoms, that are characteristic components of *P. gingivalis* lipid A.

The relationship between the chemical structure of lipid A and its endotoxic activity has been studied using both natural and chemically synthesized lipid A analogs (36, 37, 54, 55). As a tentative conclusion, the two phosphates at positions 1 and 4′ in the lipid A molecule appear to influence the activity considerably, and the degree of acylation, binding sites and type seem to be critical determinants of the potency for endotoxic activity. Taking these findings into consideration, the moderate toxicity of *P. gingivalis* LPS may originate from the low levels of acylation and phosphorylation based on heterogeneity of the lipid A part, as described above.

Recent studies have indicated that TLR4 may play an important role in LPS-mediated immune responses (4, 17, 39), and TLR2 may be associated with cellular responses to numerous microbial products (4, 53). Many preparations of LPS contain low concentrations of highly bioactive contaminants described previously as LPS protein, suggesting that these contaminants could be responsible for the TLR2-mediated signaling observed upon LPS stimulation (2, 14, 53). TNF-α production by synthetic Pg-LA and compound 506 in human monocytoid MM6-CA8 cells was significantly suppressed by the anti-human TLR4/MD-2 complex mAb (HTA125) but not by the anti-human TLR2 mAb (TL2.1), indicating that these synthetic compounds act on the cells only through the TLR4 signaling pathway. However, TL2.1 in addition to HTA125 was essential to inhibit the TNF-α-producing activity of *P. gingivalis* native lipid A. These findings indicated that both TLR2 and TLR4 pathways may be associated with the action of the native preparations on MM6-CA8 cells, in contrast to the case of synthetic analogs. Furthermore, it was also suggested that the murine TLR2 signaling pathway is associated with mitogenicity and cytokine-inductive activity by *P. gingivalis* LPS in LPS-unresponsive C3H/HeJ mice having a missense mutation in the third exon of the *TLR4* gene (39). These results indicated that the unique biological activity of *P. gingivalis* native LPS or lipid A to

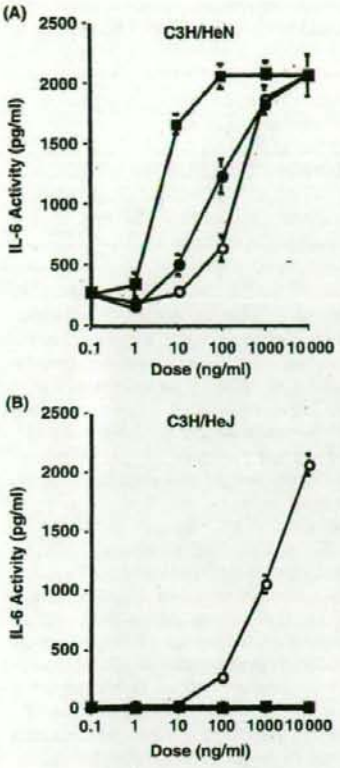


*Fig. 8.* Induction of IL-6 release from murine peritoneal macrophages from C3H/HeN and C3H/HeJ mice stimulated by *Porphyromonas gingivalis* synthetic lipid A. Stimulation of peritoneal macrophages was performed as well as that of TNF-α, and IL-6 activity in the supernatants was determined by an ELISA kit. The results are expressed as means ± SD of duplicate experiments. ●, synthetic Pg-LA; ○, native lipid A; ■, compound 506.

LPS-unresponsive mice appears to be induced by bioactive contaminants such as LPS protein (54) and other microbial components present in the native preparations. Ogawa's group recently suggested that *P. gingivalis* purified natural lipid A and compound 381 lacked the ability to activate gingival fibroblasts from C3H/HeJ, TLR4 knockout and myeloid differentiation factor 88 knockout mice (35), and also a triacylated lipoprotein, consisting of two palmitoyl groups and one pentadecanoyl group at the N-terminal of glycerocysteine from *P. gingivalis* lipid A, is a principal component for TLR2-mediated cell activation (13, 28). On the other hand, Darveau's group seem to have considered the possibility that multiple lipid A species of *P. gingivalis* may functionally interact with both TLR2 and TLR4, such as the under acylated lipid A moiety activate cells through TLR2 (6, 7).

IL-8 induction activity of synthetic Pg-LA to HGFs was significantly inhibited by polymyxin B in this study. However, no inhibitory effects of polymyxin B were observed on the immune responses of native *P. gingivalis* lipid A. The results were similar to those of other reports that the effect of polymyxin B on *P. gingivalis* LPS was relatively low (23). Polymyxin B may neutralize the endotoxicity of active-type molecules present in *P. gingivalis* LPS by binding to phosphate groups in the lipid A part (31), but may not inhibit the immune responses induced by the other contaminating bacterial components that act through the TLR2 pathway. This may be one of the reasons for the low inhibitory potency of polymyxin B to *P. gingivalis* LPS, in addition to the factors affecting the LPS-neutralization potency such as the absence of a phosphate group at position 4′ and presence of a polar head group in the native lipid A (26).

Anti-human CD14 mAb inhibited both IL-8 production from HGFs and TNF-α production from human monocytoid MM6-CA8 cells by synthetic Pg-LA as described in this study. On the other hand, it has been reported that anti-murine CD14 mAb could block *P. gingivalis* LPS-mediated immune responses (50) that may be mediated through both TLR2 and TLR4. These findings suggested that CD14 associates closely with not only the TLR4 but also the TLR2 signaling pathway mediated by *P. gingivalis* LPS. This was also supported by our previous report (54) that the LPS-antagonist, succinylated lipid A precursor (succinylated 406), inhibited TNF-α induction activity of *P. gingivalis* native lipid A in peritoneal macrophages from C3H/HeN and C3H/HeJ mice. In addition B464, a low-toxicity lipid A analog (62), significantly inhibited TNF-α production from human monocytoid MM6-CA8 cells induced by *P. gingivalis* native and synthetic lipid A (data not shown). Succinylated 406 and B464 competitively inhibit LPS action at the same stages in the LPS signaling pathway involving LBP, CD14 and TLRs. Taking these points into consideration, both LPS inhibitors appear to suppress the immune responses through CD14 and the TLR family including TLR2, by blocking the function of CD14 in the signaling cascade.

In conclusion, these findings suggested that the moderated and reduced biological activity of *P. gingivalis* LPS and native lipid A, including the activity on C3H/HeJ mouse cells via the TLR2-mediated pathway, may be mediated by bioactive contaminants or low acylated molecules present in the native preparations having high heterogeneity in lipid A moiety. To elucidate these problems, we are now attempting to evaluate the biological characterizations of tetra-acylated monophosphorylated or diphosphorylated species with the predominant molecules found in *P. gingivalis* native lipid A, using each chemically synthesized analog.

## Acknowledgments

We would like to thank Dr Shoichi Kusumoto for helpful advice in the synthesis process of lipid A. We would also like to thank Drs Toshimi Murai and Yukari Nakagawa for helpful advice on the culture method of MM6-CA8 cells and Daiichi Pharmaceutical Co. for providing *Escherichia coli*-type synthetic lipid A (compound 506). This work was supported in part by grants from the Ministry of Education,

*Table 3.* Effects of mAbs on the production of TNF-α by human monocytoid MM6-CA cells stimulated with *P. gingivalis* synthetic lipid A

| | Stimulants *P. gingivalis* lipid A | | | | | |
|---|---|---|---|---|---|---|
| | Native | | Synthetic | | Compound 506 | |
| mAbs | TNF-α release[1] | % control | TNF-α release[1] | % control | TNF-α release[1] | % control |
| Non | 118.0 ± 2.1 | 100.0 | 428.6 ± 45.6 | 100.0 | 420.8 ± 48.9 | 100.0 |
| Anti-TLR2 | 65.0 ± 3.0 | 55.1 | 398.2 ± 89.5 | 92.9 | 396.0 ± 22.2 | 94.1 |
| Anti-TLR4 | 67.0 ± 0.2 | 56.8 | 5.7 ± 3.1 | 1.3 | 11.5 ± 3.6 | 2.7 |
| Anti-TLR2 + TLR4 | 35.0 ± 3.6 | 29.7 | 18.2 ± 7.8 | 4.2 | 40.3 ± 5.6 | 9.6 |
| Anti-CD14 | 38.0 ± 2.1 | 32.2 | 3.8 ± 1.2 | 0.9 | 3.4 ± 1.1 | 0.8 |

[1]TNF-α release in pg/ml. Dose of each antibody: anti-human TLR2 mAb TL2.1, 5 μg/ml; anti-human TLR4/MD-2 complex mAb HTA125, 5 μg/ml; anti-human CD14 mAb MY4, 10 μg/ml. Dose of each lipid: *Porphyromonas gingivalis* native lipid A, 10 ng/ml; *P. gingivalis* synthetic lipid A, 1 ng/ml; compound 506, 1 ng/ml.

Science and Culture (17592170 to H.K. and 04671111 to Y.H.)

## References


1. Abreu MT, Fukata M, Arditi M. TLR signaling in the gut in health and disease. J Immunol 2005: **174**: 4453–4460.
2. Aliprantis AO, Yang RB, Mark MR et al. Cell activation and apoptosis by bacterial lipoproteins through toll-like receptor-2. Science 1999: **285**: 736–739.
3. Al-Qutub MN, Braham PH, Karimi-Naser LM, Liu X, Genco CA, Darveau RP. Hemin-dependent modulation of the lipid A structure of *Porphyromonas gingivalis* lipopolysaccharide. Infect Immun 2006: **74**: 4474–4485.
4. Anderson KV. Toll signaling pathways in the innate immune response. Curr Opin Immunol 2000: **12**: 13–19.
5. Burgess K, Jennings LD. Enantioselective esterifications of unsaturated alcohols mediated by a lipase prepared from *Pseudomonas* sp. J Am Chem Soc 1991: **113**: 6129–6139.
6. Darveau RP, Pham TT, Lemley K et al. *Porphyromonas gingivalis* lipopolysaccharide contains multiple lipid A species that functionally interact with both Toll-like receptors 2 and 4. Infect Immun 2004: **72**: 5041–5051.
7. Dixon DR, Darveau RP. Lipopolysaccharide heterogeneity: innate host responses to bacterial modification of lipid A structure. J Dent Res 2005: **84**: 584–595.
8. Fujiwara T, Ogawa T, Sobue S, Hamada S. Chemical, immunobiological and antigenic characterizations of lipopolysaccharides from *Bacteroides gingivalis* strains. J Gen Microbiol 1990: **136**: 319–326.
9. Fukase K, Kurosawa S, Kusumoto S. Synthesis and purification by HPLC of de-*O*-acyl partial structures of *Escherichia coli* Re lipopolysaccharide. J Endotoxin Res 1994: **1**: 149–163.
10. Galanos C, Lüderitz O, Westphal O. Preparation and properties of a standardized lipopolysaccharide from *Salmonella abortus equi*. Zentralbl Bakteriol (Orig A) 1979: **243**: 226–244.
11. Guo L, Lim KB, Gunn JS et al. Regulation of lipid A modifications by *Salmonella typhimurium* virulence genes phoP-phoQ. Science 1997: **276**: 250–253.
12. Hamada S, Takada H, Mihara J, Nakagawa I, Fujiwara T. LPS of oral *Bacteroides* species: general properties and induction of cytokines in human gingival fibroblast cultures. In: Nowotny A, Spitzer JJ, Ziegler EJ, ed. Cellular and molecular aspects of endotoxin reactions. Amsterdam: Elsevier Science Publishers, 1990: 285–294.
13. Hashimoto M, Asai Y, Ogawa T. Separation and structural analysis of lipoprotein in a lipopolysaccharide preparation from *Porphyromonas gingivalis*. Int Immunol 2004: **16**: 1431–1437.
14. Hirschfeld M, Ma Y, Weis JH, Vogel SN, Weis JJ. Repurification of LPS eliminates signaling through both human and murine Toll-like receptor 2. J Immunol 2000: **165**: 618–622.
15. Holt SC, Ebersole J, Felton J, Brunsvold M, Kornman S. Implantation of *Bacteroides gingivalis* in nonhuman primates initiates progression of periodontitis. Science 1988: **239**: 55–57.
16. Homma JY, Matsuura M, Kanegasaki S et al. Structural requirements of lipid A responsible for the functions: a study with chemically synthesized lipid A and its analogues. J Biochem 1985: **98**: 395–406.
17. Hoshino K, Takeuchi O, Kawai T et al. Toll-like receptor 4 (TLR4)-deficient mice are hyporesponsive to lipopolysaccharide: evidence for TLR4 as the Lps gene product. J Immunol 1999: **162**: 3749–3752.
18. Iino Y, Hopes RM. The bone resorbing activities in tissue culture of lipopolysaccharides from the bacteria *Actinobacillus actinomycetemcomitans*, *Bacteroides gingivalis*, and *Capnocytophaga ochracea* isolated from human mouths. Arch Oral Biol 1984: **29**: 59–63.
19. Imoto M, Yoshimura H, Shimamoto T, Sakaguchi N, Kusumoto S, Shiba T. Total synthesis of *Escherichia coli* lipid A, the endotoxically active principle of cell-surface lipopolysaccharide. Bull Chem Soc Jpn 1987: **60**: 2205–2214.
20. Inage M, Chaki H, Imoto M, Shimamoto T, Kusumoto S, Shiba T. Synthetic approach to lipid As: preparation of phosphorylated disaccharides containing (*R*)-3-hydroxyacyl and (*R*)-3-acyloxyacyl groups. Tetrahedron Lett 1983: **24**: 2011.
21. Kato H, Haishima Y, Iida T, Tanaka A, Tanamoto K. Chemical structure of lipid A isolated from *Flavobacterium meningosepticum* lipopolysaccharide. J Bacteriol 1998: **180**: 3891–3899.
22. Kawahara K, Tsukano H, Watanabe H, Lindner B, Matsuura M. Modification of the structure and activity of lipid A in *Yersinia pestis* lipopolysaccharide by growth temperature. Infect Immun 2002: **70**: 4092–4098.
23. Kirikae T, Nitta T, Kirikae F et al. Lipopolysaccharides (LPS) of oral black-pigmented bacteria induce tumor necrosis factor production by LPS-refractory C3H/HeJ macrophages in a way different from that of *Salmonella* LPS. Infect Immun 1999: **67**: 1736–1742.
24. Koga T, Nishihara T, Fujiwara T et al. Biochemical and immunobiological properties of lipopolysaccharide (LPS) from *Bacteroides gingivalis* and comparison with LPS from *Escherichia coli*. Infect Immun 1985: **47**: 638–647.
25. Kumada H, Haishima Y, Kondo S, Umemoto T, Hisatsune K. Occurrence of 2-keto-3-deoxyoctonate (KDO) and KDO phosphate in lipopolysaccharides of *Bacteroides* species. Curr Microbiol 1993: **26**: 239–244.
26. Kumada H, Haishima Y, Umemoto T, Tanamoto K. Structural study on the free lipid A isolated from lipopolysaccharide of *Porphyromonas gingivalis*. J Bacteriol 1995: **177**: 2098–2106.
27. Kumada H, Watanabe K, Umemoto T, Kato K, Kondo S, Hisatsune K. Chemical and biological properties of lipopolysaccharide, lipid A and degraded polysaccharide from *Wolinella recta* ATCC 33238. J Gen Microbiol 1989: **135**: 1017–1025.
28. Makimura Y, Asai Y, Taiji Y, Sugiyama A, Tamai R, Ogawa T. Correlation between chemical structure and biological activities of *Porphyromonas gingivalis* synthetic lipopeptide derivatives. Clin Exp Immunol 2006: **146**: 159–168.
29. Mansheim BJ, Onderdonk AB, Kasper DL. Immunochemical and biological studies of the lipopolysaccharide of *Bacteroides melaninogenicus* subspecies *asaccharolyticus*. J Immunol 1978: **120**: 72–78.
30. Medzhitov R, Preston-Hurlburt P, Janewy CA Jr. A human homologue of the *Drosophila* Toll protein signals activation of adaptive immunity. Nature 1997: **388**: 394–397.
31. Morrison DC, Danner RL, Dinarello CA et al. Bacterial endotoxins and pathogenesis of Gram-negative infections: current status and future direction. J Endotoxin Res 1994: **1**: 71–83.
32. Nair BC, Mayberry WR, Dziak R, Chen PB, Levine MJ, Hausmann E. Biological effects of a purified lipopolysaccharide from *Bacteroides gingivalis*. J Periodontal Res 1983: **18**: 40–49.
33. Nashed MA, Anderson L. Iodine as a reagent for the ready hydrolysis of prop-1-enyl glycosides, or their conversion into oxazolines. J Chem Soc Chem Commun 1982: **21**: 1274–1276.
34. Obayashi T, Tamura H, Tanaka S et al. A new chromogenic endotoxin-specific assay using recombined limulus coagulation enzymes and its clinical applications. Clin Chim Acta 1985: **149**: 55–65.
35. Ogawa T, Asai Y, Hashimoto M et al. Cell activation by *Porphyromonas gingivalis* lipid A molecule through Toll-like receptor 4- and myeloid differentiation factor 88- dependent signaling pathway. Int Immunol 2002: **14**: 1325–1332.
36. Ogawa T, Asai Y, Yamamoto H et al. Immunobiological activities of a chemically synthesized lipid A of *Porphyromonas gingivalis*. FEMS Immunol Med Microbiol 2000: **28**: 273–281.
37. Ogawa T, Uchida H, Amino K. Immunobiological activities of chemically defined lipid A from lipopolysaccharides of *Porphyromonas gingivalis*. Microbiology 1994: **140**: 1209–1216.
38. Oltvoort JJ, Van Boeckel CAA, De Koning JH, Van Boom JH. Use of the cationic iridium complex 1,5-cyclooctadiene-bis[methyldiphenylphosphine]-iridium hexa fluorophosphate in carbohydrate chemistry: smooth isomerization of allyl ethers to 1-propenyl ethers. Synthesis 1981: **1981**: 305–308.
39. Poltorak A, He X, Smirnova I et al. Defective LPS signaling in C3H/HeJ and C57BL/10ScCr mice: mutations in *Tlr4* gene. Science 1998: **282**: 2085–2088.
40. Qureshi N, Takayama K. Purification and structural determination of nontoxic lipid A obtained from the lipopolysaccharide of *Salmonella typhimurium*. J Biol Chem 1982: **257**: 11808–11815.
41. Qureshi N, Takayama K, Meyer KC et al. Chemical reduction of 3-oxo and unsaturated

groups in fatty acids of diphosphoryl lipid A from the lipopolysaccharide of *Rhodopseudomonas sphaeroides*. J Biol Chem 1991: **266**: 6532–6538.
42. Rietschel ET, Brade L, Schade U et al. Bacterial endotoxins: properties and structure of biologically active domains. In: Schrinner E, Richmond MH, Seibert G, Schwarz U, ed. Surface structures of microorganisms and their interactions with the mammalian host. Weinheim, Germany: VCH Verlagsgesellschaft mbH, 1988: 1–41.
43. Rosenstreich DL, Glode LM. Differences in B cell mitogen responsiveness between closely related strains of mice. J Immunol 1975: **115**: 777–780.
44. Schifferle RE, Reddy MS, Zambon JJ, Genco RJ, Levine MJ. Characterization of a polysaccharide antigen from *Bacteroides gingivalis*. J Immunol 1989: **143**: 3035–3042.
45. Shimazu R, Akashi S, Ogata H et al. MD-2, a molecule that confers lipopolysaccharide responsiveness on Toll-like receptor 4. J Exp Med 1999: **189**: 1777–1782.
46. Skidmore BJ, Morrison DC, Chiller JM, Weigle WO. Immunologic properties of bacterial lipopolysaccharide (LPS). II. The unresponsiveness of C3H/HeJ mouse spleen cells to LPS-induced mitogenesis is dependent on the method used to extract LPS. J Exp Med 1975: **142**: 1488–1508.
47. Slots J, Genco RJ. Microbial pathogenicity. Black pigmented *Bacteroides* species, *Capnocytophaga* species, and *Actinobacillus actinomycetemcomitans* in human periodontal disease: virulence factors in colonization, survival, and tissue destruction. J Dent Res 1984: **63**: 412–421.
48. Soejima K, Ishizaka A, Urano T et al. Protective effect of B464, a lipid A analog, on endotoxin-induced cellular responses and acute lung injury. Am J Resp Crit Care Med 1996: **154**: 900–906.
49. Suda Y, Kirikae T, Shiyama T et al. Macrophage activation in response to S-form lipopolysaccharides (LPS) separated by centrifugal partition chromatography from wild-type LPS: effects of the *O*-polysaccharide portion of LPS. Biochem Biophys Res Commun 1995: **210**: 678–685.
50. Tabeta K, Yamazaki K, Akashi S et al. Toll-like receptors confer responsiveness to lipopolysaccharide from *Porphyromonas gingivalis* in human gingival fibroblasts. Infect Immun 2000: **68**: 3731–3735.
51. Takada H, Mihara J, Morisaki I, Hamada S. Induction of interleukin-1 and -6 in human gingival fibroblast cultures stimulated with *Bacteroides* lipopolysaccharides. Infect Immun 1991: **59**: 295–301.
52. Takeda K, Akira S. Toll-like receptors in innate immunity. Int Immunol 2005: **17**: 1–14.
53. Takeuchi O, Hoshino K, Kawai T et al. Differential roles of TLR2 and TLR4 in recognition of gram-negative and gram-positive bacterial cell wall components. Immunity 1999: **11**: 443–451.
54. Tanamoto K, Azumi S, Haishima Y, Kumada H, Umemoto T. The lipid A moiety of *Porphyromonas gingivalis* lipopolysaccharide specifically mediates the activation of C3H/HeJ mice. J Immunol 1997: **158**: 4430–4436.
55. Tanamoto K, Azumi S, Haishima Y, Kumada H, Umemoto T. Endotoxic properties of free lipid A from *Porphyromonas gingivalis*. Microbiology 1997: **143**: 63–71.
56. Tanamoto K, Kato H, Haishima Y, Azumi S. Biological properties of lipid A isolated from *Flavobacterium meningosepticum*. Clin Diagn Lab Immunol 2001: **8**: 522–527.
57. Urban FJ, Moore BS, Breitenbach R. Synthesis of tigogenyl β-*O*-cellobioside heptaacetate and glycoside tetraacetate via Schmidt's trichloroacetimidate method: some new observations. Tetrahedron Lett 1990: **31**: 4421–4424.
58. Westphal O, Lüderitz O, Bister R. Über die Extraction von Bakterien mit Phenol/Wasser. Z Naturforsch (Tiel B) 1952: **7**: 148–155.
59. Wilson M. Biological activities of lipopolysaccharide and endotoxin. In: Haroun HN, ed. Biology of the species *Porphyromonas gingivalis*. Boca Raton, FL: CRC Press, 1993: 171–198.
60. Winkelhoff AJ, Steenbergen TJM, Graaff J. Occurrence and association with disease. In: Haroun HN. ed. Biology of the Species Porphyromonas gingivalis. Boca Raton, Florida: CRC Press, 1993: 33–44.
61. Yamaji Y, Kubota T, Sasaguri K et al. Inflammatory cytokine gene expression in human periodontal ligament fibroblasts stimulated with bacterial lipopolysaccharides. Infect Immun 1995: **63**: 3576–3581.
62. Zeigler-Heitbrock HW, Thiel E, Futterer A, Herzog V, Wirtz A, Riethmuller G. Establishment of a human cell line (Mono Mac 6) with characteristics of mature monocytes. Int J Cancer 1988: **41**: 456–461.